Exclusive π^- Asymmetry Studies

M. Kerr, T. Hayward, H. Avakian

June 30, 2026 | CLAS Collaboration Meeting

CEBAF Large Acceptance Spectrometer

Motivations

- Using various deeply virtual meson production (DVMP) processes, we can probe ***chiral odd GPDs***
  - Chiral odd GPDs much less understood and quantified than chiral even counterparts probed using DVCS and similar processes
- RG-C longitudinally polarized ND_3 target allows us to study ***beam*** (A_{LU}), ***target*** (A_{UL}), and ***double*** (A_{LL}) spin asymmetries, probing combinations of GPD contributions using five modulation terms
  - $A_{LU}^{\sin\phi}, A_{UL}^{\sin\phi}, A_{UL}^{\sin 2\phi}, A_{LL}^{\cos 0\phi}, A_{LL}^{\cos\phi}$
- Nuclear target → effects of Fermi motion
- First DVπ^-P studies from CLAS12
  - Complementary to RG-C exclusive π^+ analysis now in analysis review stage
  - Simultaneous studies of RG-B exclusive π^- beam spin asymmetry, to either complete separately or combine with RG-C exclusive π^- beam spin asymmetry results

		Quark Polarization		
		Unpolarized (U)	Longitudinally Polarized (L)	Transversely Polarized (T)
Nucleon Polarization	U	H		$2\widetilde{H}_T + E_T$
	L		$\widetilde{H}$	$\widetilde{E}_T$
	T	E	$\widetilde{E}$	$H_T, \widetilde{H}_T$

chiral odd GPDs

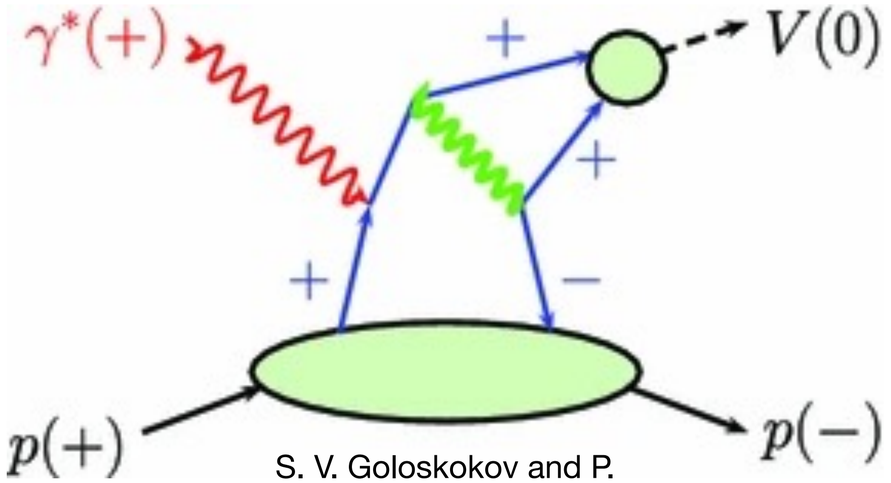

S. V. Goloskokov and P. Kroll, *Eur. Phys. J. C*, vol. 74, p. 2725, 2014.

General Information on Analysis

1. RG-C
   - In-bending data from existing run periods: Su22, Fa22, Sp23
     - Fa22 has flip in solenoid settings: before (“Pre-SF”) and after (“Post-SF”) analyzed separately
   - Longitudinally polarized ND_3 target, neutrons of interest to scatter off in bound deuteron state
   - Data from a collection of targets (C, CH_2/ CD_2, He, ET) used to quantify effects of nuclear target through ***packing fraction*** and ***dilution factor***
2. RG-B
   - Analyzing in-bending data collected from Sp19 run period (pass2)
   - Unpolarized LD_2 target

Binning Choices

- 1D bins in x_B and $-t'$ for beam, target, double spin asymmetries; 2D bins in $(x_B, -t')$ for beam spin asymmetry as uncertainties smaller (not handling target polarization)
  - $t' = t - t_{min}$
- Increased statistics of RG-B Sp19 reflected in smaller 1D bins

1. 1D in x_B:
   - RG-B $\rightarrow x_B \in [0.085, 0.15, 0.2, 0.25, 0.3, 0.35, 0.4, 0.45, 0.5, 0.55, 0.6)$
   - RG-C $\rightarrow x_B \in [0.085, 0.2, 0.3, 0.4, 0.5, 0.6)$
2. 1D in $-t'$:
   - RG-B $\rightarrow -t' \in [0.05, 0.15, 0.25, 0.35, 0.45, 0.55, 0.65, 0.75, 0.85, 0.95, 1.05, 1.15, 1.25)$ GeV^2
   - RG-C $\rightarrow -t' \in [0.05, 0.25, 0.45, 0.65, 0.85, 1.05, 1.25)$ GeV^2
3. 2D:
   - RG-B/C $\rightarrow x_B \in [0.085, 0.2, 0.3, 0.4, 0.5, 0.6)$ and $-t' \in [0.05, 0.25, 0.45, 0.65, 0.85, 1.05, 1.25)$ GeV^2

Two versus Three Particle Final State

- For exclusive π^+ studies, channel is $ep \rightarrow en\pi^+ \rightarrow$ analysis is done using two particle (e, π^+) final state due to low efficiency neutron detection
- Exclusive π^- studies ($en \rightarrow ep\pi^-$), have a higher complete final state yield because of higher efficiency proton detection $\rightarrow$ two (e, π^-) or three (e, π^-, p) particle final state possible to analyze
- Two particle final state still has higher statistics but higher likelihood for contamination from background, Fermi motion
- Sufficient statistics from three particle final state so currently focusing on this method!

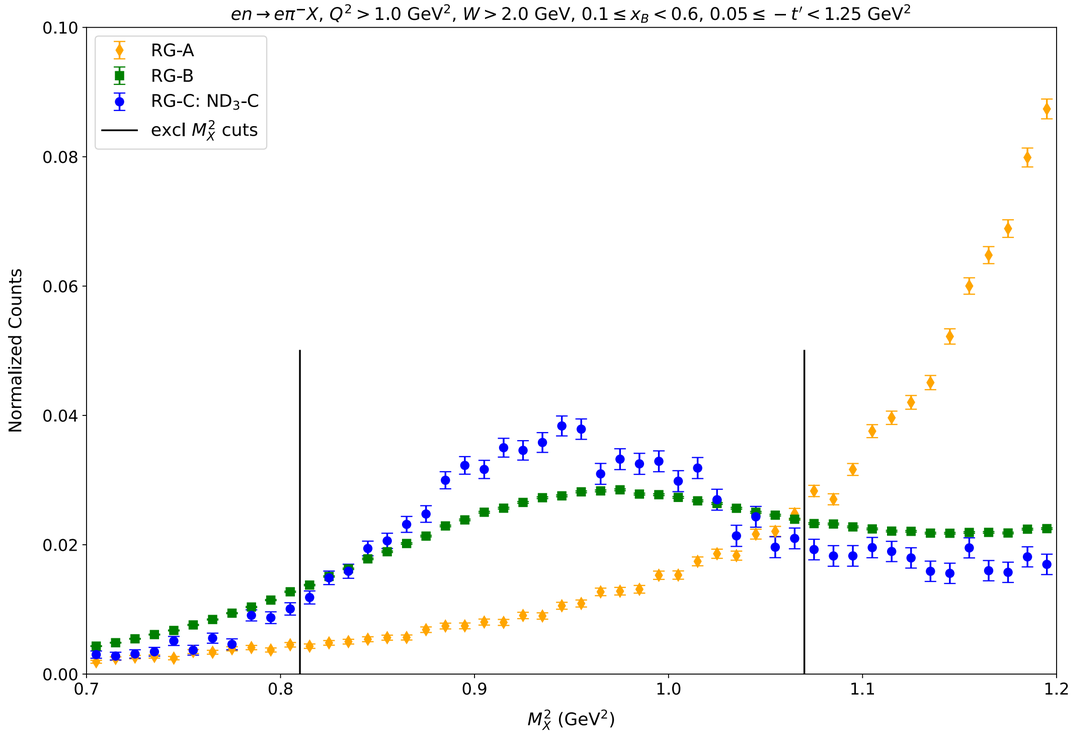

$en \rightarrow e\pi^-X$

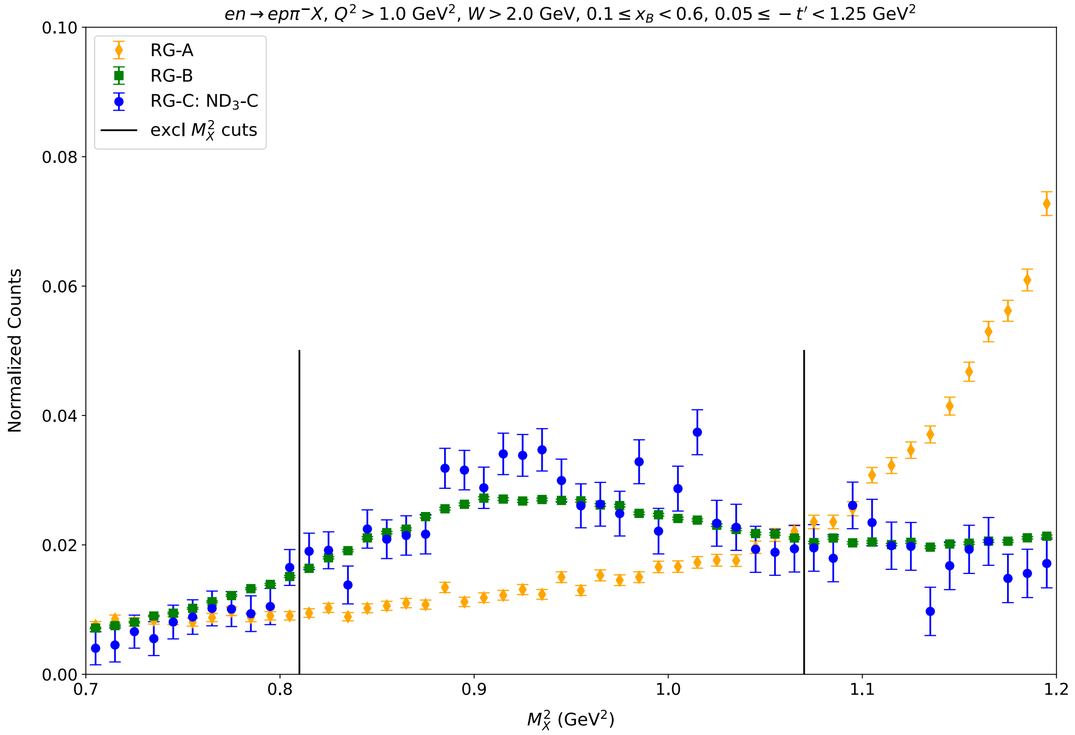

$en \rightarrow ep\pi^-X$

Missing Mass and Momentum Cuts

- With three particle final state, use bound state of protons and neutrons in deuterium to improve missing cuts
  - Setting the target mass to mass of deuteron, $M_d \sim 1.875$ GeV so missing 4 vector reconstructs the observer nucleon in the deuteron bound state
- Initial procedure:
  1. ***Fit M_X^2 distribution using Gaussian + polynomial, accepting missing mass range to be $\mu \pm 2\sigma$***
  2. Construct p_X distribution events passing M_X^2 cuts. Fit again using Gaussian + polynomial, and again accept missing momentum range $\mu \pm 2\sigma$

Other cuts:

- $Q^2 > 1$ GeV^2, $W > 2$ GeV, $y < 0.8$
- EventBuilder PID
- Loose vertex cuts on detected e^-
- QADB
- $0.085 \leq x_B < 0.6$, 0.05 GeV$^2 \leq -t' < 1.25$ GeV^2

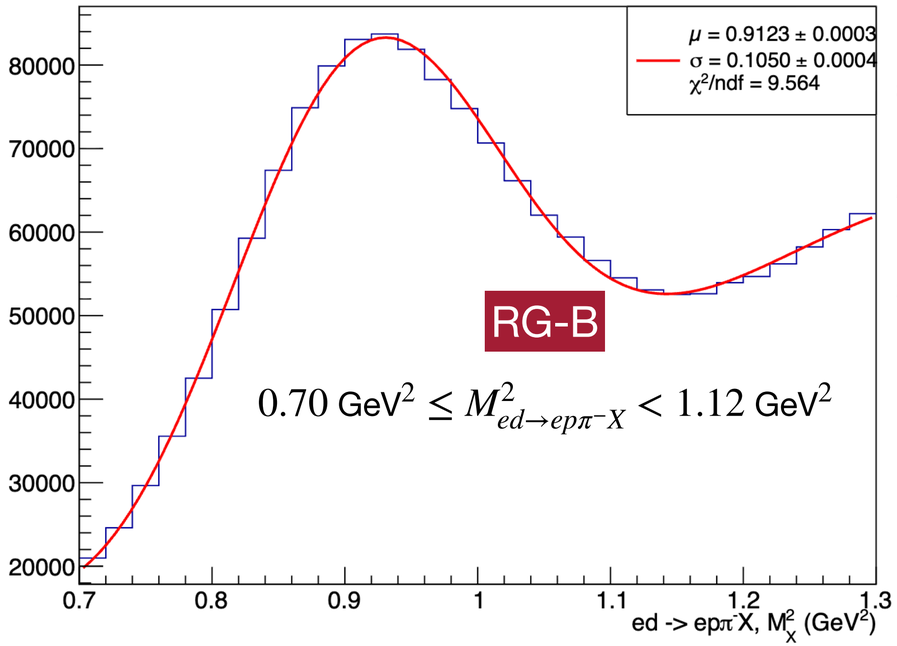

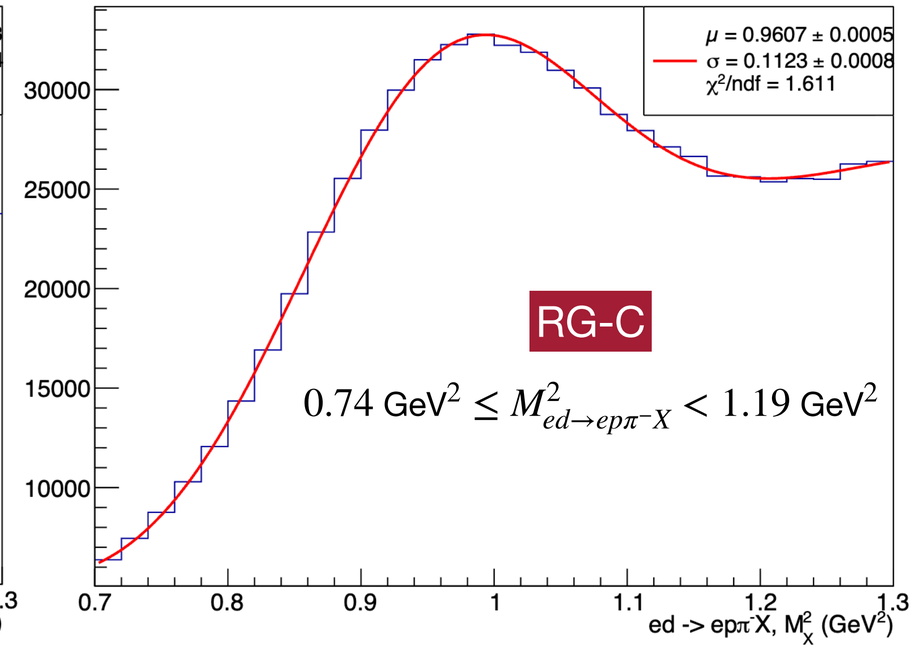

RG-C peak wider due to heightened Fermi motion

Missing Mass and Momentum Cuts

- With three particle final state, use bound state of protons and neutrons in deuterium to improve missing cuts
  - Setting the target mass to mass of deuteron, $M_d \sim 1.875$ GeV so missing 4 vector reconstructs the observer nucleon in the deuteron bound state
- Initial procedure:
  1. Fit M_X^2 distribution using Gaussian + polynomial, accepting missing mass range to be $\mu \pm 2\sigma$
  2. ***Construct p_X distribution events passing M_X^2 cuts. Fit again using Gaussian + polynomial, and again accept missing momentum range $\mu \pm 2\sigma$***

Other cuts:

- $Q^2 > 1$ GeV^2, $W > 2$ GeV, $y < 0.8$
- EventBuilder PID
- Loose vertex cuts on detected e^-
- QADB
- $0.085 \leq x_B < 0.6$, 0.05 GeV$^2 \leq -t' < 1.25$ GeV^2

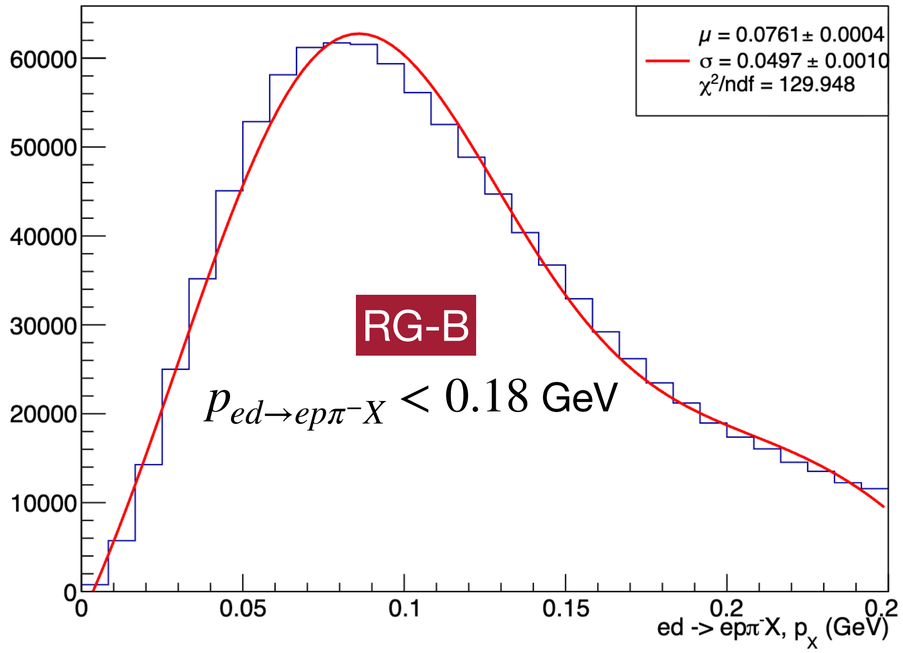

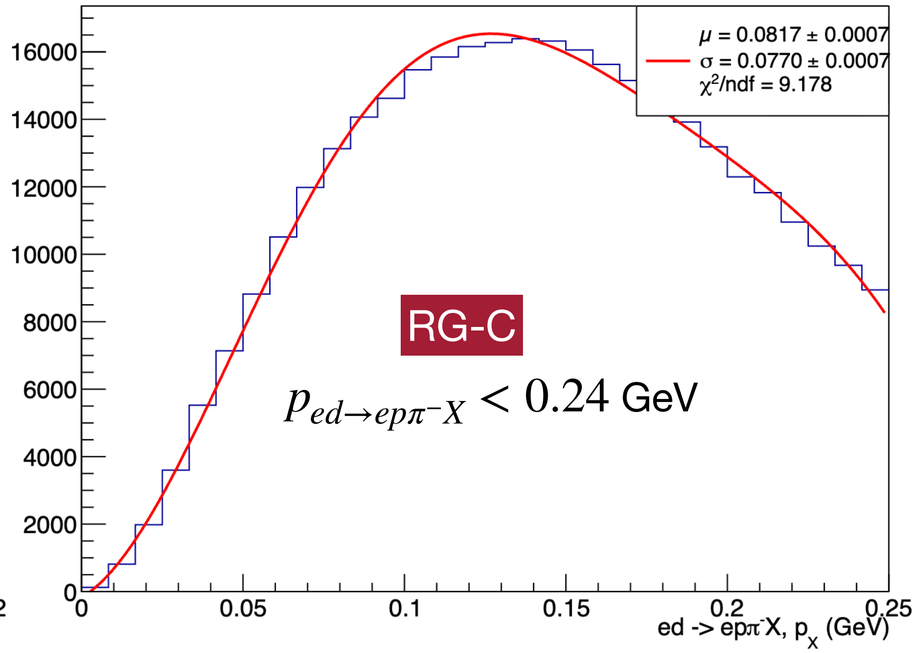

RG-C peak wider due to heightened Fermi motion

RG-C Quantification of Nuclear Target Contributions

- Dilution factor scales results to reflect polarized components of target
- Enters as a scaling factor in target and double spin asymmetries

Dilution factor, packing fraction calculations, and methodology by Sebastian Kuhn and Derek Holmberg, https://clasweb.jlab.org/wiki/images/5/52/RG-C_Dilution_v3.1.1.pdf

$n_A \rightarrow$ (polarized) ND_3

$n_{MT} \rightarrow He$

$n_{CD} \rightarrow CD_2$

$n_C \rightarrow C$

$n_F \rightarrow$ Foils (completely empty target)

$$DF = \frac{(n_A - n_{MT})\,(n_{CD} - 0.757666 n_C - 0.005200 n_{MT} - 0.237132 n_F)}{n_A\,(n_{CD} - 0.168370 n_C - 0.865973 n_{MT} + 0.03434 n_F)}$$

$$PF = 0.442453 \frac{n_A - n_{MT}}{n_{CD} - 0.168370 n_C - 0.865973 n_{MT} + 0.03434 n_F}$$

- Measures of how tightly molecules are “packed” into the target cell
- Should be uniform across processes → useful for comparison
- Can also be used to construct dilution factor, yielding a near identical result with somewhat higher uncertainty

$CH_2 \rightarrow CD_2$ Conversion Technique for RG-C Su22 and Fa22

- Sp23 only RG-C run period with data off entire target set for dilution factor
  - Su22 & Fa22 missing data off of CD_2 target so manipulation required to calculate these dilution factors

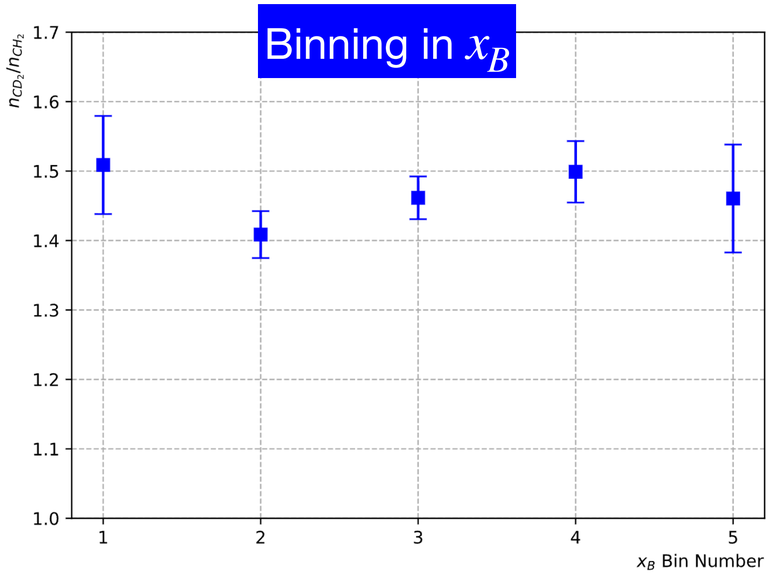

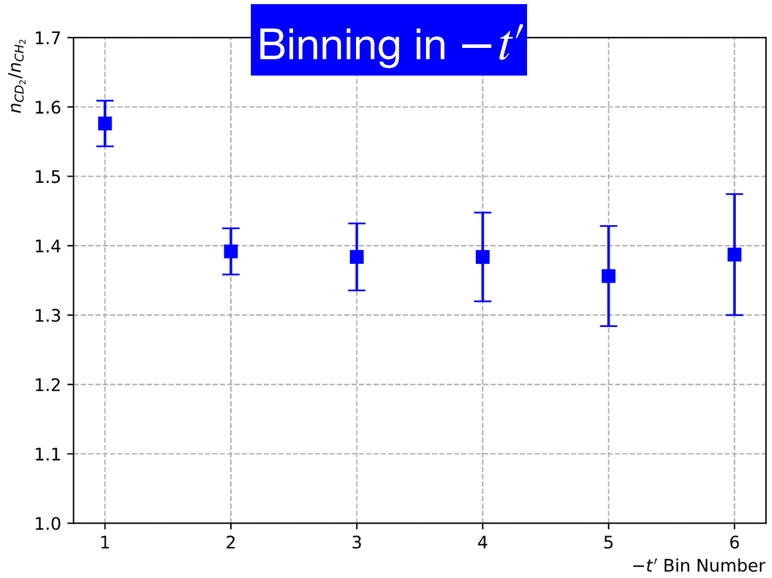

Relatively consistent ratios across kinematic bins

1. Calculate charge-normalized counts per kinematic bin for Sp23 CH_2 and CD_2 targets
2. Construct ratio (per kinematic bin) of CH_2 to CD_2 using Sp23 data
3. Apply ratio to charge-normalized counts per kinematic bin of Su22, Fa22 CH_2 data

→ Despite missing CD_2 data in two periods, we can manipulate CH_2 data to still analyze full RG-C ND_3 dataset

RG-C Packing Fraction

- In general, good agreement between run periods binned both in x_B and $-t'$ and stability of packing fraction result across kinematics as desired
- Also, good agreement between mean values of packing fractions calculated over all kinematics in three run periods:
  1. Summer 2022: $\langle Pf \rangle = 0.4842 \pm 0.0187$
  2. Fall 2022: $\langle Pf \rangle = 0.5099 \pm 0.0158$
  3. Spring 2023: $\langle Pf \rangle = 0.4812 \pm 0.0087$

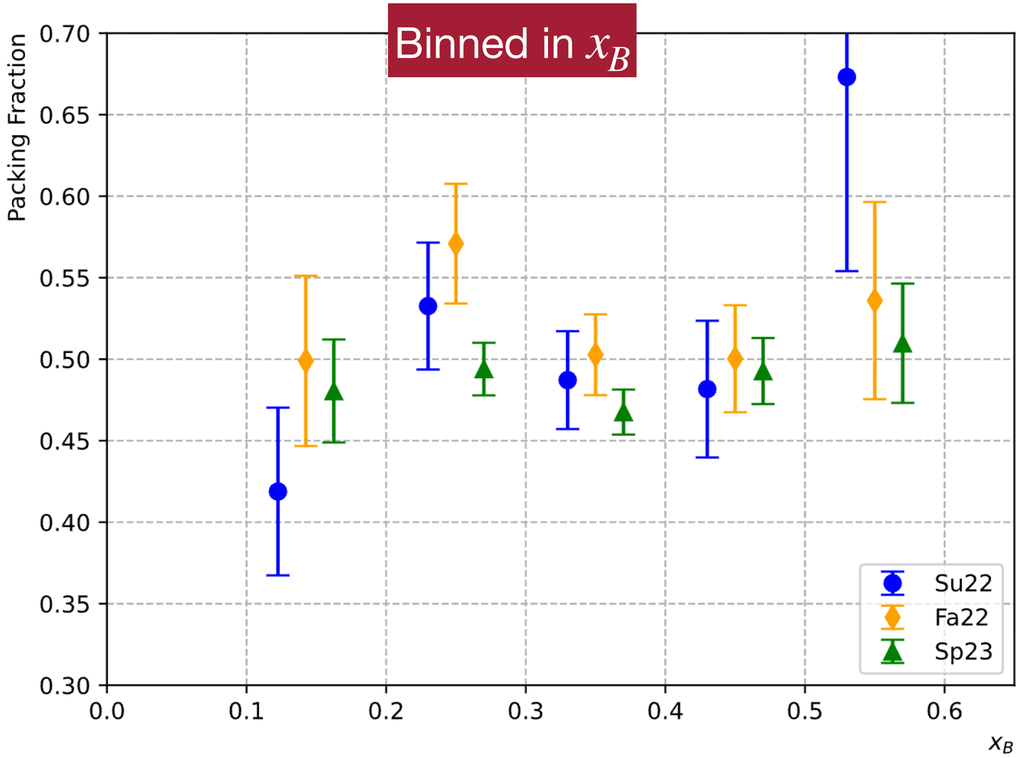

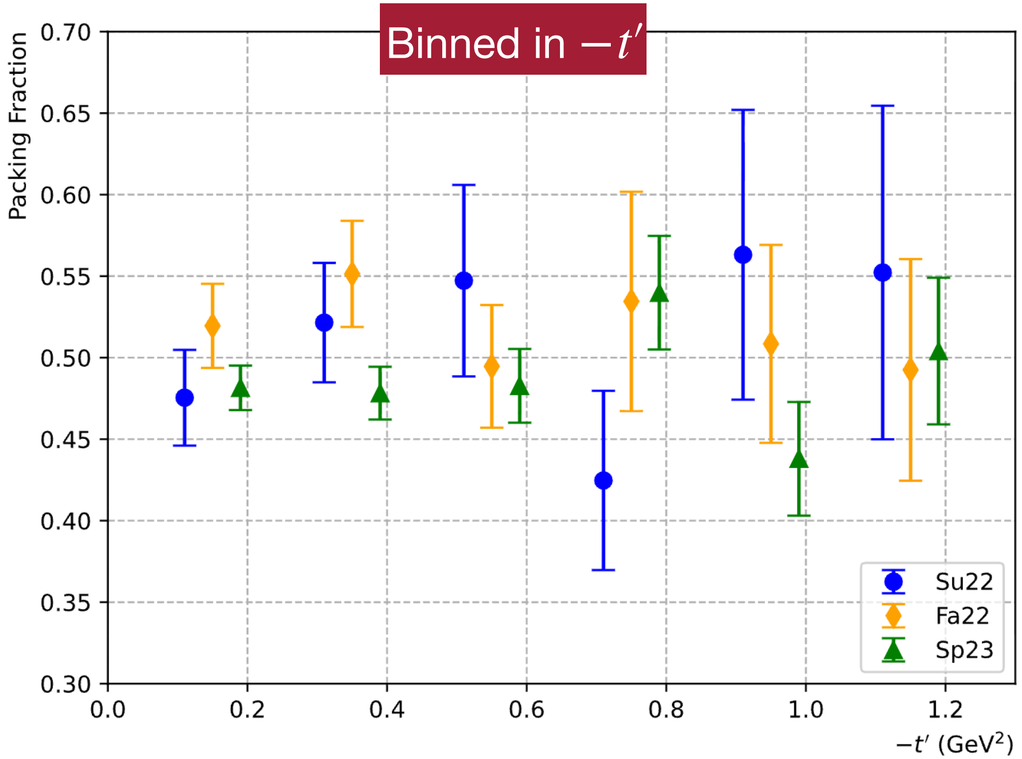

RG-C Dilution Factor

- Good agreement between run periods binned both in x_B and $-t'$ and excellent agreement between mean values of dilution factors calculated over all kinematics in three run periods:
  1. Summer 2022: $\langle Df \rangle = 0.4598 \pm 0.0118$
  2. Fall 2022: $\langle Df \rangle = 0.4533 \pm 0.0080$
  3. Spring 2023: $\langle Df \rangle = 0.4540 \pm 0.0082$
- Dilution factor for exclusive π^+ is $\sim 0.4 \rightarrow$ higher dilution factor expected for these studies as we are detecting complete final state
  - Results suggest we are doing a good job at selecting exclusive π^- events from neutron in deuteron bound state

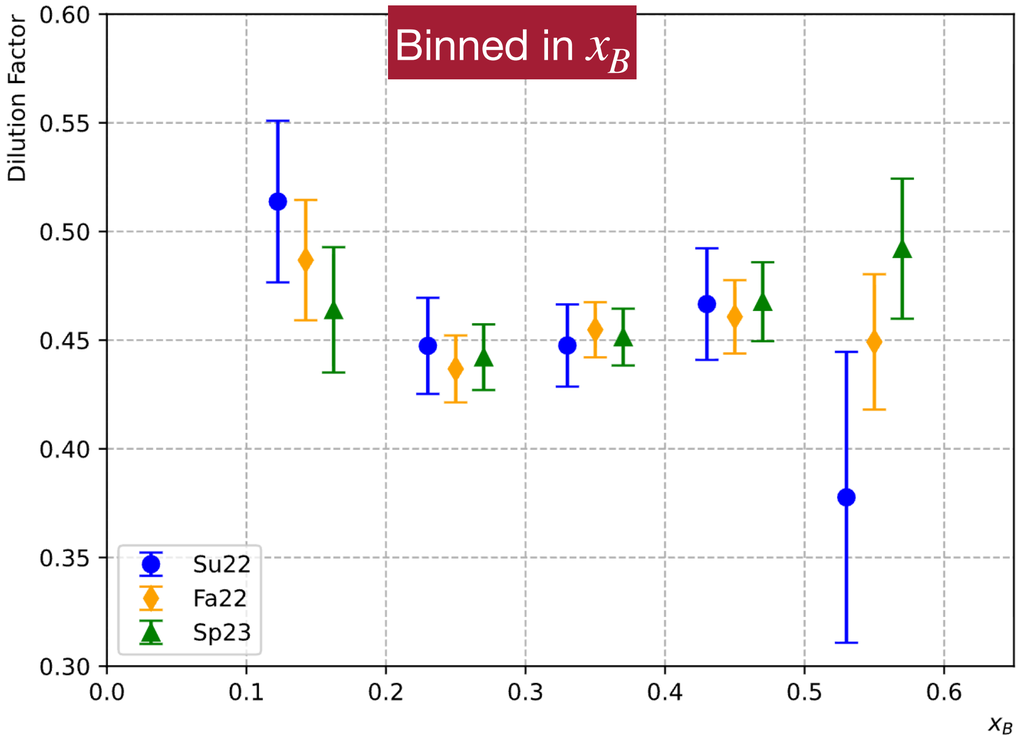

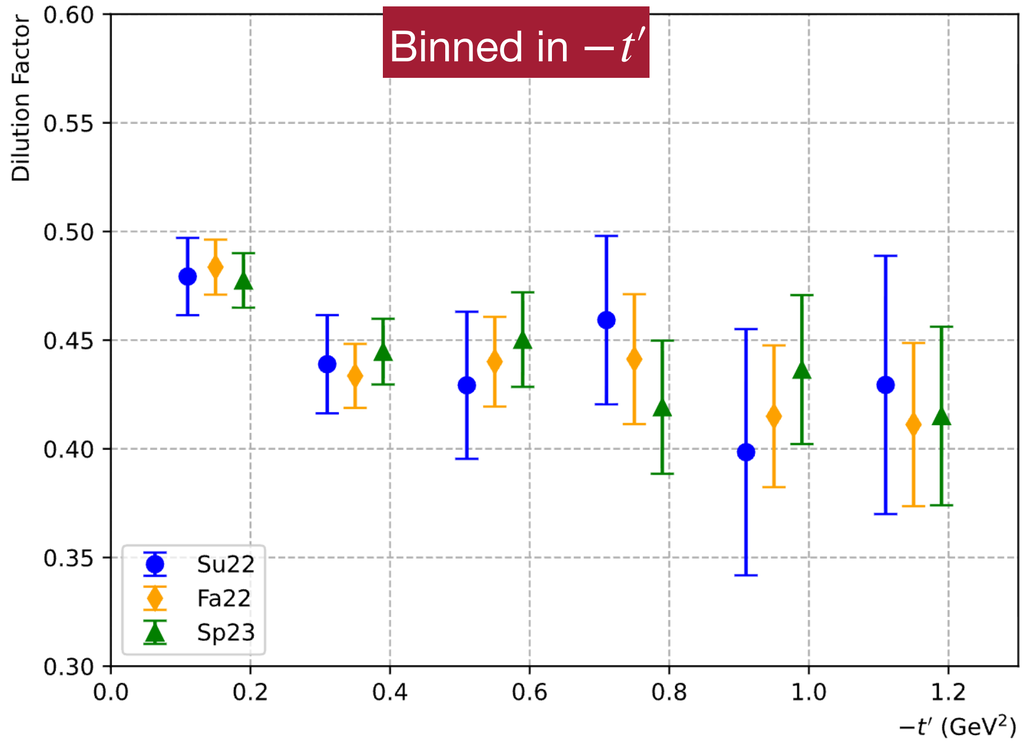

Beam Spin Asymmetry Extraction

$$A_{LU} = \frac{1}{P_b}\frac{N^+ - N^-}{N^+ + N^-}$$

$$A_{LU}(\phi) = c_0 + A_{LU}^{\sin\phi}\sin\phi$$

- $N^{\pm}$ corresponds to number of counts with positive (negative) beam helicity
- Does not require normalization because of consistent CEBAF beam helicity flipping

Run Period	P_b
RG-B Sp19	0.848 ± 0.009*
RG-C Su22	0.8384 ± 0.0086
RG-C Fa22	0.8372 ± 0.0045
RG-C Sp23	0.8040 ± 0.0061

*Average value

RG-B Sp19

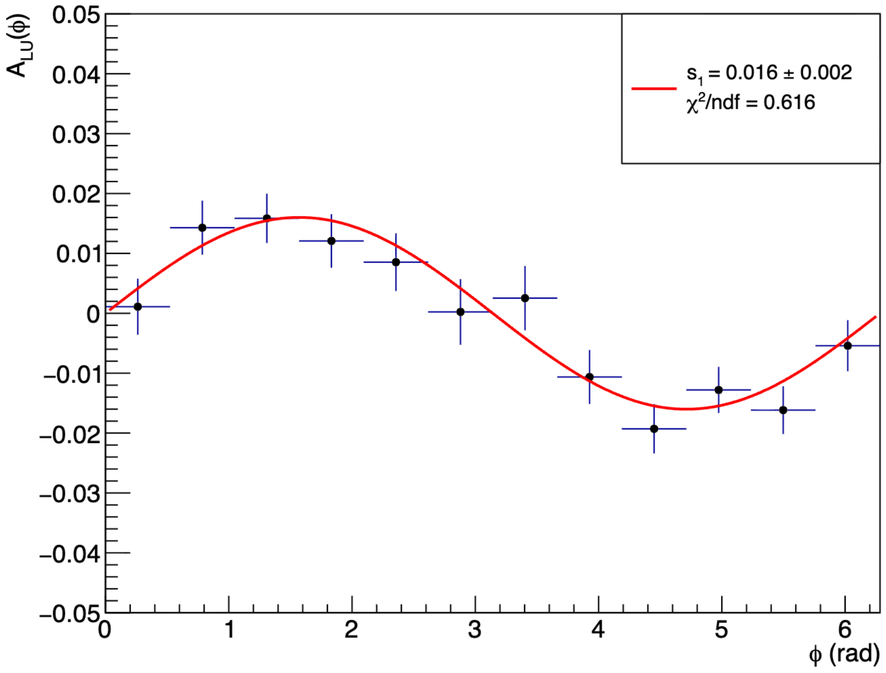

RG-C Fa22 Pre-SF

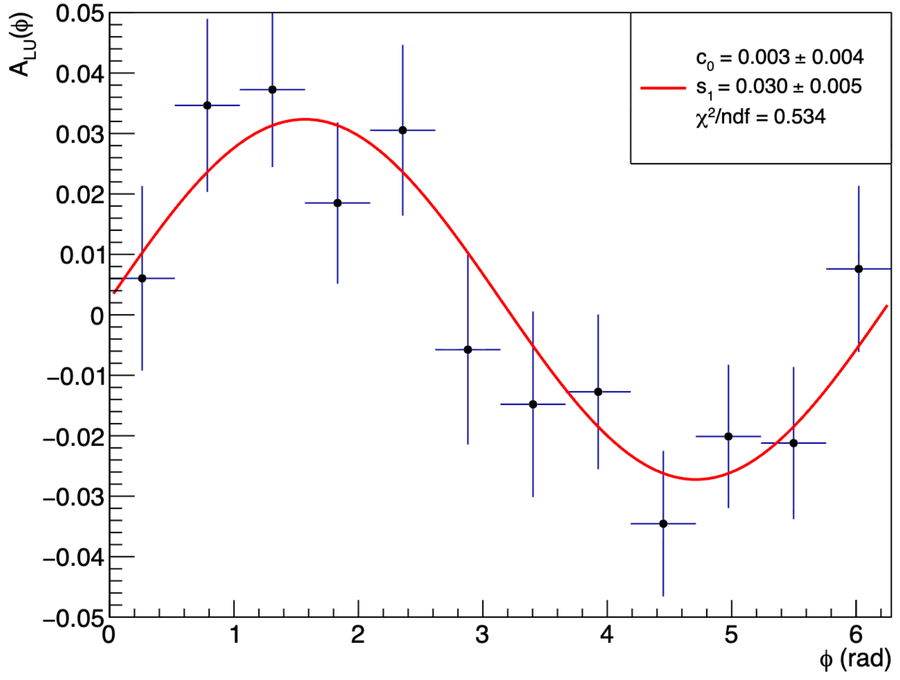

- Integrated kinematic space: $0.085 \leq x_B < 0.6$, $0.05\ \text{GeV}^2 \leq -t' < 1.25\ \text{GeV}^2$
- $A_{LU}^{\sin\phi}$ amplitudes relatively small → result of positive and negative asymmetries when considering kinematic dependence
- RG-C amplitudes consistently $> 1\sigma$ larger than RG-B → may be handled in structure function result by including depolarization factor

$A_{LU}^{\sin\phi}$ for 1D x_B and 1D $-t'$ Binning

- Agreement between RG-B and RG-C improves with binning → seems to be the worst at high x_B. RG-C internal run periods in general have good agreement
- For binning in x_B, $A_{LU}^{\sin\phi}$ is low/possibly negative small x_B but increases proportionally with x_B
- Interesting dependence here in $-t'$, where $A_{LU}^{\sin\phi}$ is smallest and dipping negative at mid range in $-t'$, $-t' \sim 0.7$ GeV^2, while lower and higher regions in $-t'$ are have larger, positive $A_{LU}^{\sin\phi}$

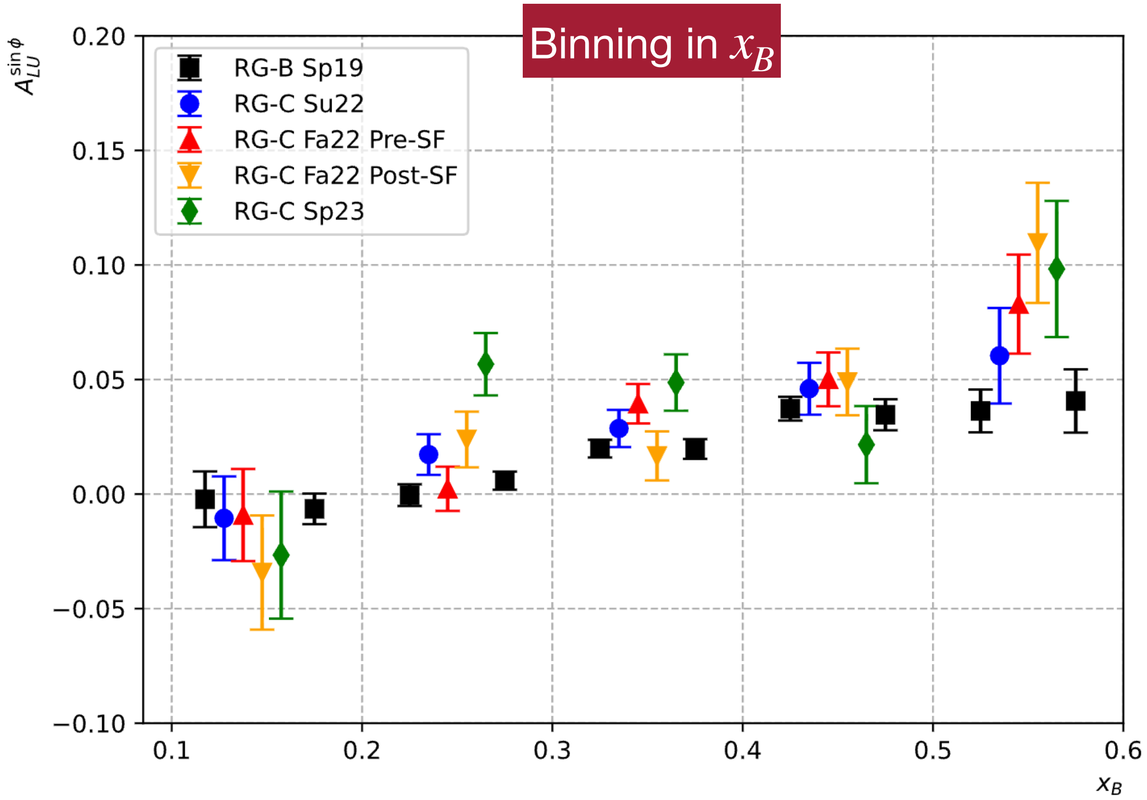

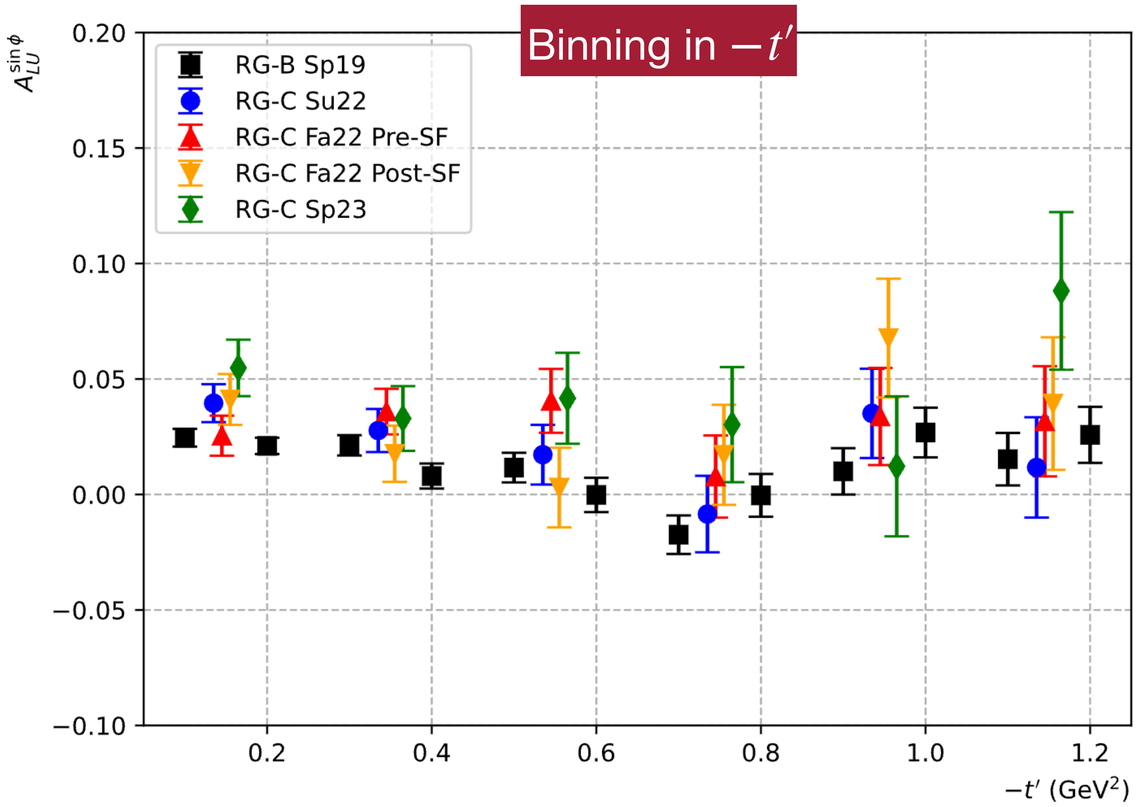

$A_{LU}^{\sin\phi}$ binned in 2D $(x_B, -t')$

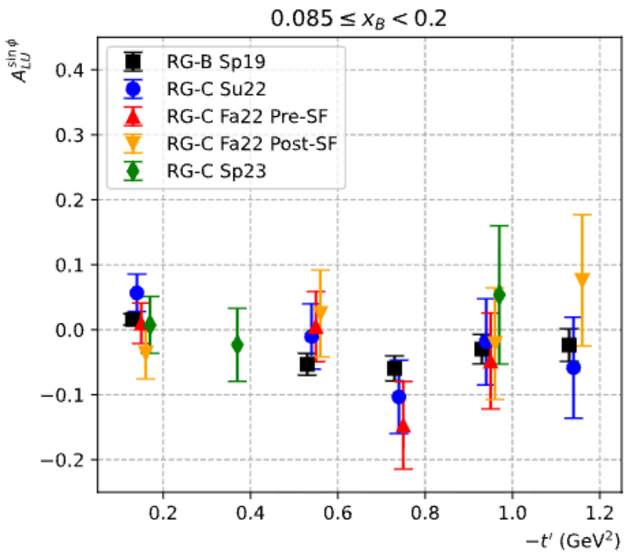

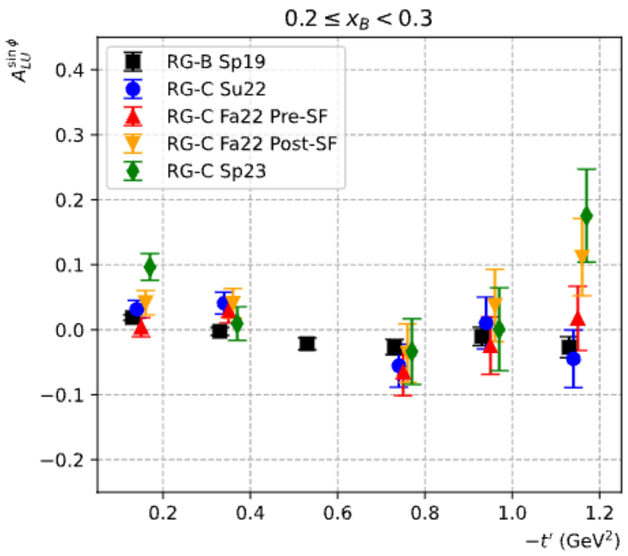

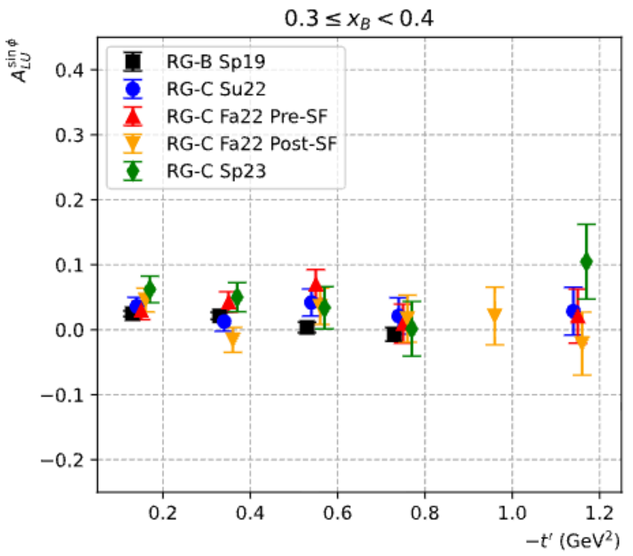

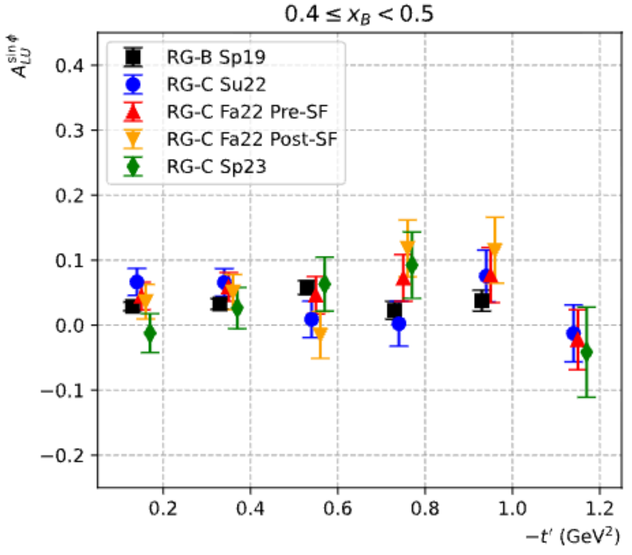

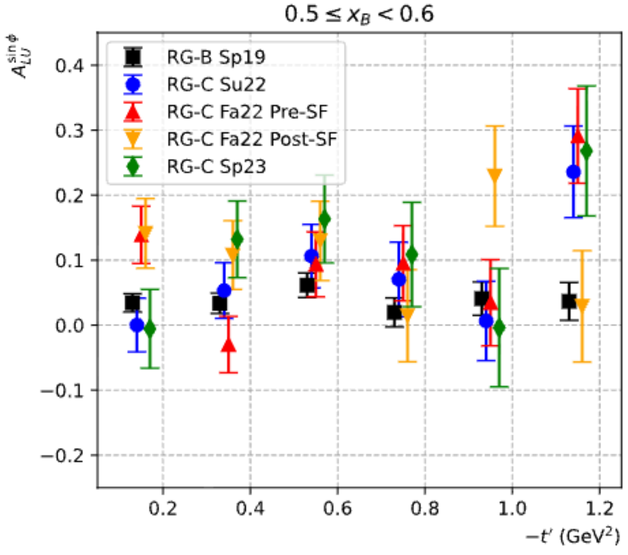

Comparing to RG-C exclusive π^+ $F_{LU}^{\sin\phi}/F_{UU}$, π^- results are consistently smaller, and include negative $A_{LU}^{\sin\phi}$ fit regions which are not apparent in π^+ results.

- Binning in 2D unlocks negative $A_{LU}^{\sin\phi}$ fit regions more clearly → in particular at low x_B and high $-t'$
- Agreement between RG-C and RG-B mostly still good, worst at high x_B
- Some fits do not converge → merging RG-C run periods and possibly reducing number of bins may help with this

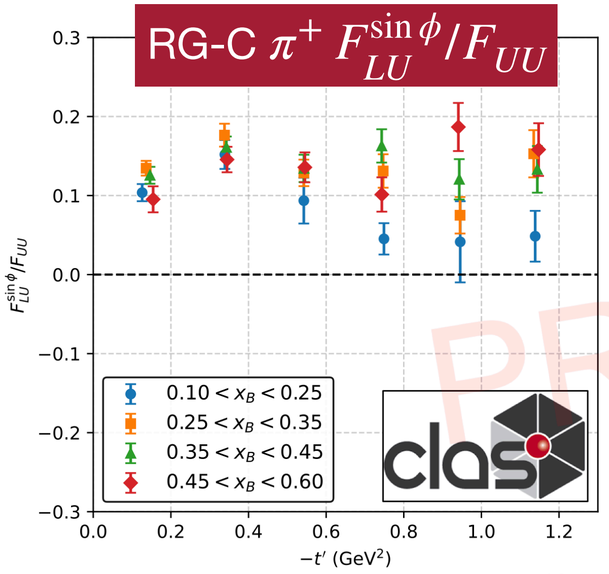

Target Spin Asymmetry Extraction

$$A_{UL} = \frac{1}{Df} \frac{n^+ - n^-}{P_t^- n^+ + P_t^+ n^-}$$

$$A_{UL}(\phi) = c_0 + A_{UL}^{\sin\phi} \sin\phi + A_{UL}^{\sin 2\phi} \sin 2\phi$$

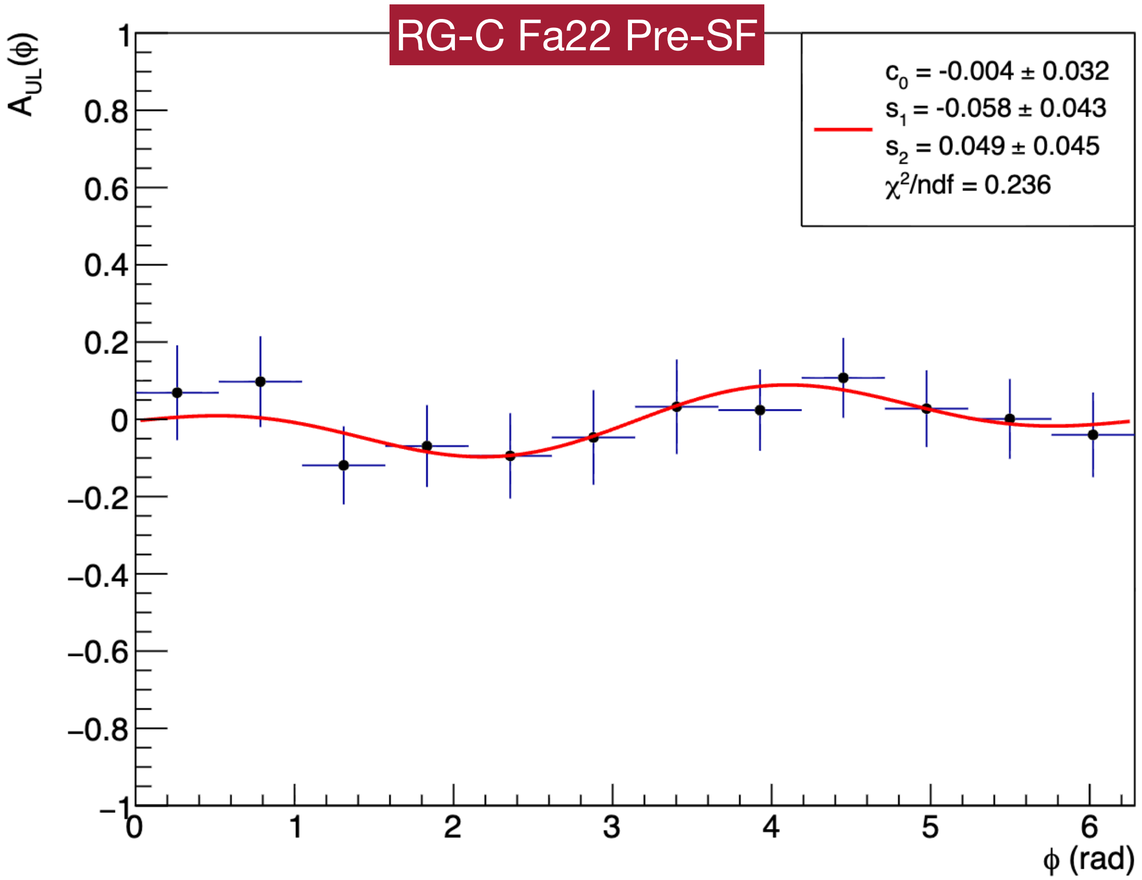

- $n^{\pm}$ corresponds to normalized number of counts with positive (negative) target polarization
- Normalization to ensures number of counts is consistent between target polarization states; otherwise there will be a constant offset from zero in fitting (sine modulations should remain the same)
- Normalizing to number of counts integrated across ϕ in a given kinematic bin: $n^{\pm}(\phi) = N^{\pm}(\phi) / \sum_{\phi} N^{\pm}(\phi)$

Run Period	P_t^+	P_t^-
RG-C Su22	0.215 ± 0.024	0.179 ± 0.024
RG-C Fa22 Pre-SF	0.275 ± 0.024	0.239 ± 0.024
RG-C Fa22 Post-SF	0.215 ± 0.036	0.299 ± 0.048
RG-C Sp23	0.236 ± 0.025	0.223 ± 0.037

Target polarization determined by elastic analysis done by Noémie Pilleux, https://clasweb.jlab.org/wiki/index.php/File:RGC_meeting_March3.pdf

$A_{UL}^{\sin\phi}$ for 1D x_B and 1D $-t'$ Binning

- Now seeing good agreement between run periods for one dimensional binning
- Large uncertainties currently makes results difficult to fully interpret, but due to the good agreement results may be more clear after combining run periods
- One notable result from the RG-C π^+ studies is the negative $A_{UL}^{\sin\phi}$ result at low x_B, which agrees with low statistics observation from HERMES of large negative $A_{UL}^{\sin\phi}$ in exclusive region for π^+ (and for π^-, with possible ρ contamination)
- Conversion from $A_{UL}^{\sin\phi}$ to structure function divides amplitude by factor of $\sim 1.8 \rightarrow$ we observe (with large uncertainty) a seemingly *similarly negative* $A_{UL}^{\sin\phi}$ from exclusive π^- at low x_B

Binning in x_B

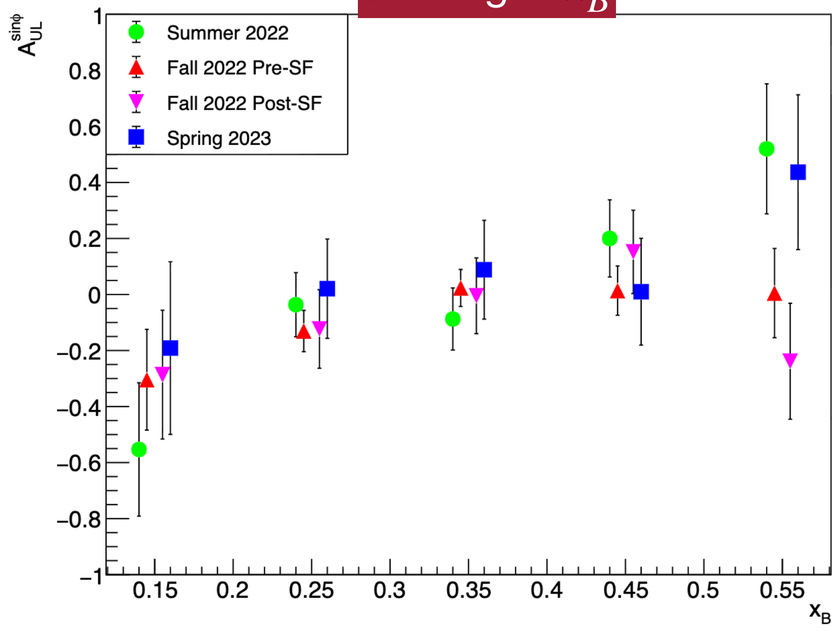

Binning in $-t'$

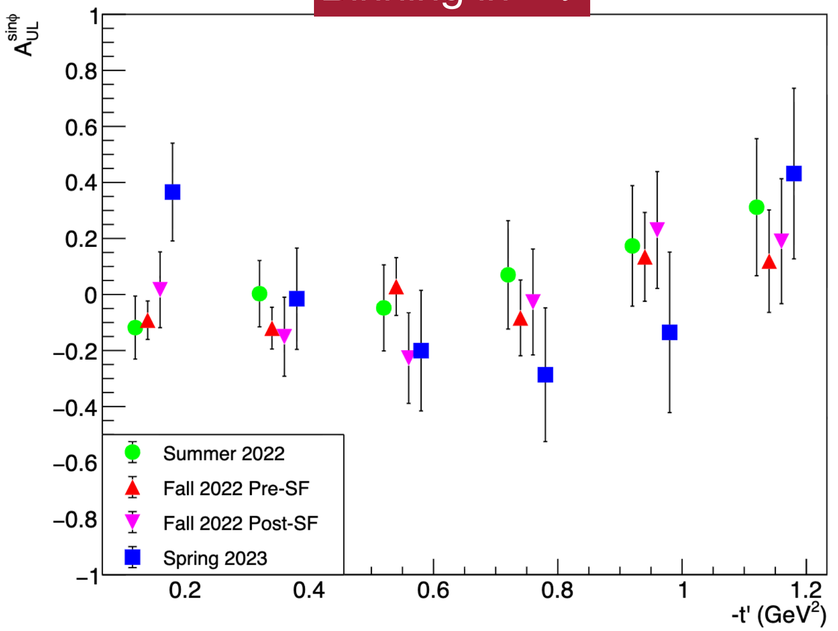

RG-C π^+ $F_{UL}^{\sin\phi}/F_{UU}$

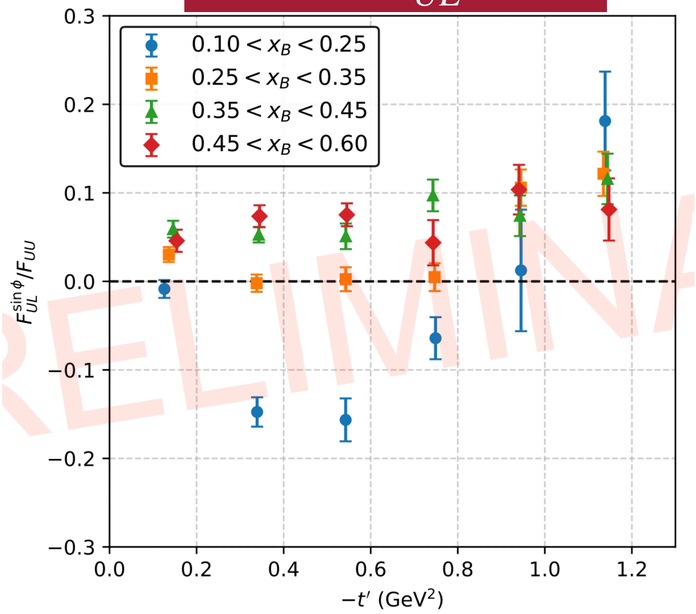

$A_{UL}^{\sin 2\phi}$ for 1D x_B and 1D $-t'$ Binning

- Also now seeing good agreement between run periods for one dimensional binning
- Large uncertainties currently makes results difficult to fully interpret, but due to the good agreement results may be more clear after combining run periods → currently nearly all the bins are consistent with zero within uncertainty for all run periods
- Unlike $\pi^+ A_{UL}^{\sin 2\phi}$, it does not appear that the $\pi^- A_{UL}^{\sin 2\phi}$ has large negative amplitude anywhere in (one-dimensional) phase space → possibly slightly negative at large x_B and low $-t'$

Binning in x_B

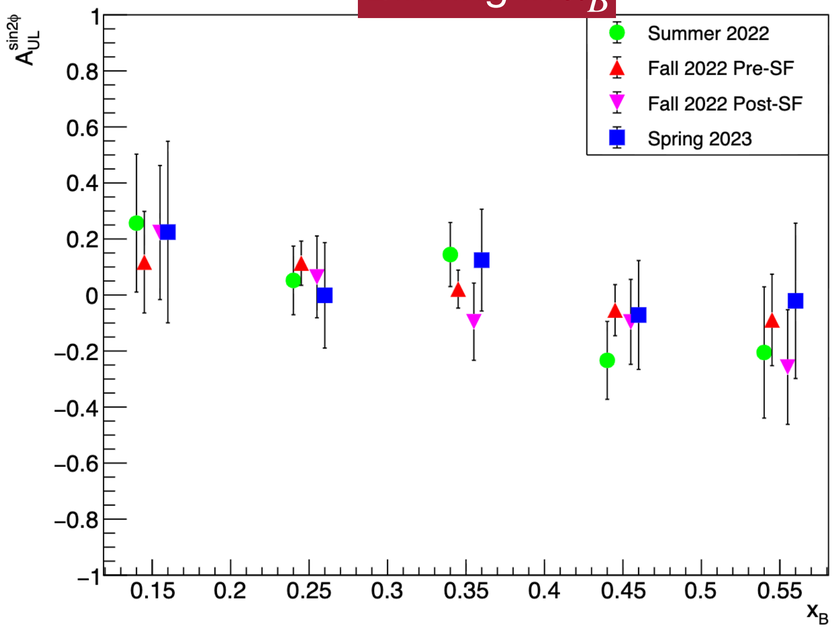

Binning in $-t'$

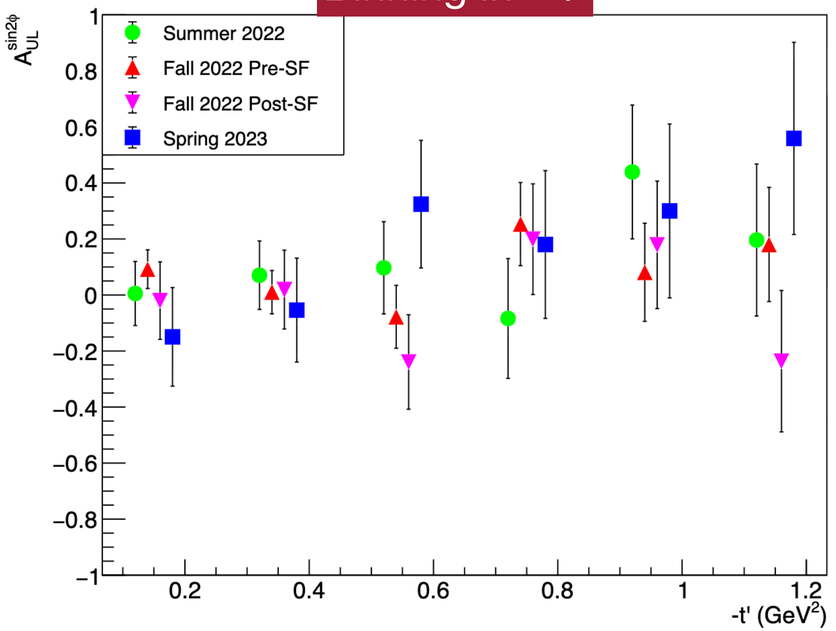

RG-C $\pi^+ F_{UL}^{\sin 2\phi}/F_{UU}$

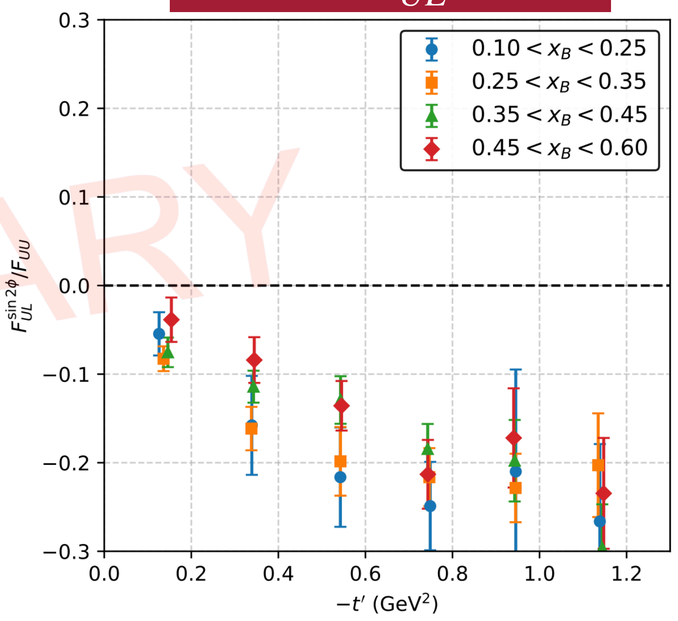

Double Spin Asymmetry Extraction

$$A_{UL} = \frac{1}{P_b D f} \frac{n^{++} - n^{-+} + n^{--} - n^{+-}}{P_t^-(n^{++} + n^{-+}) + P_t^+(n^{--} + n^{+-})}$$

$$A_{LL}(\phi) = A_{LL}^{\cos 0\phi} + A_{LL}^{\cos \phi} \cos \phi$$

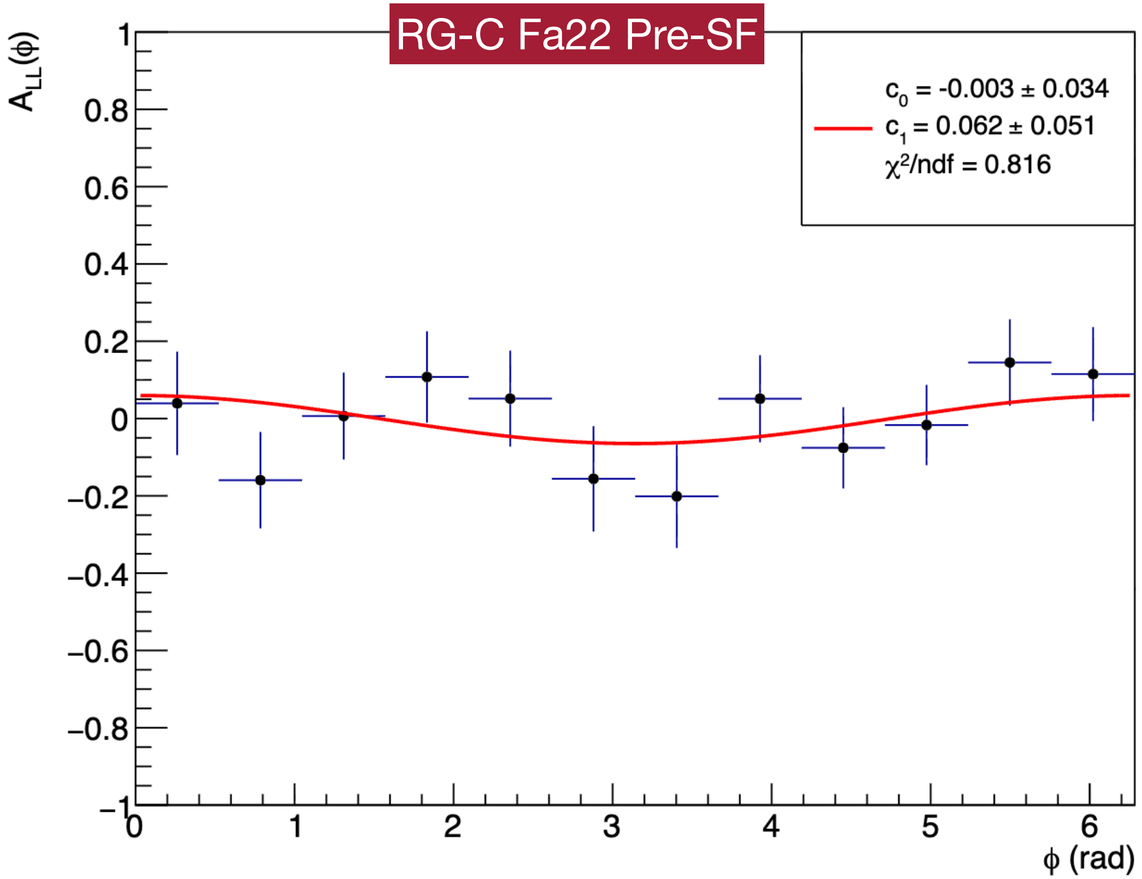

- $n^{\pm\pm} \rightarrow n^{bt}$, corresponding to normalized number of counts with positive (negative) beam polarization b and positive (negative) target polarization t
- Normalization very important as $A_{LL}^{\cos 0\phi}$ term contains physics (not just a constant offset)
- Normalizing to number of counts integrated across ϕ in a given kinematic bin:
  $n^{bt}(\phi) = N^{bt}(\phi) / \sum_{\phi} N^{bt}(\phi)$

Run Period	P_b
RG-C Su22	0.8384 ± 0.0086
RG-C Fa22	0.8372 ± 0.0045
RG-C Sp23	0.8040 ± 0.0061

Run Period	P_t^+	P_t^-
RG-C Su22	0.215 ± 0.024	0.179 ± 0.024
RG-C Fa22 Pre-SF	0.275 ± 0.024	0.239 ± 0.024
RG-C Fa22 Post-SF	0.215 ± 0.036	0.299 ± 0.048
RG-C Sp23	0.236 ± 0.025	0.223 ± 0.037

$A_{LL}^{\cos 0\phi}$ for 1D x_B and 1D $-t'$ Binning

Binning in x_B

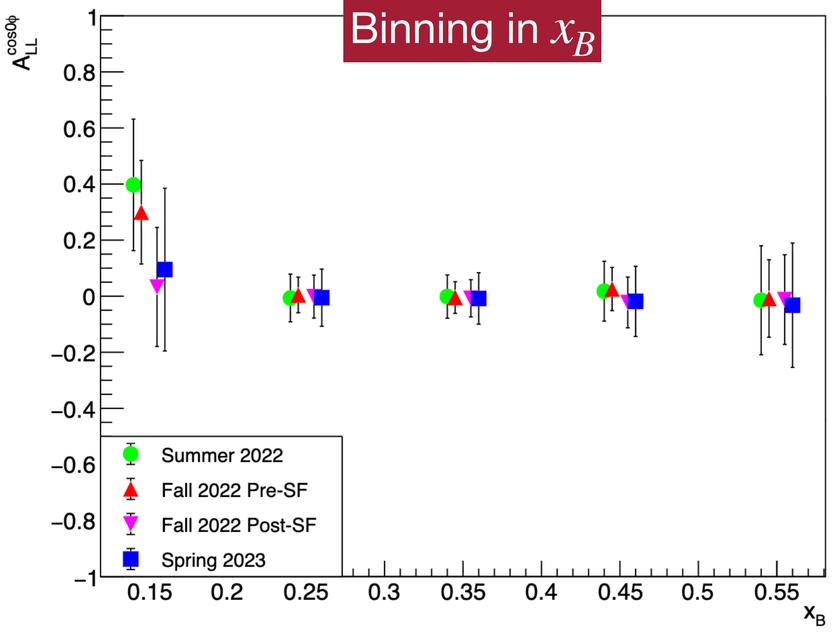

Binning in $-t'$

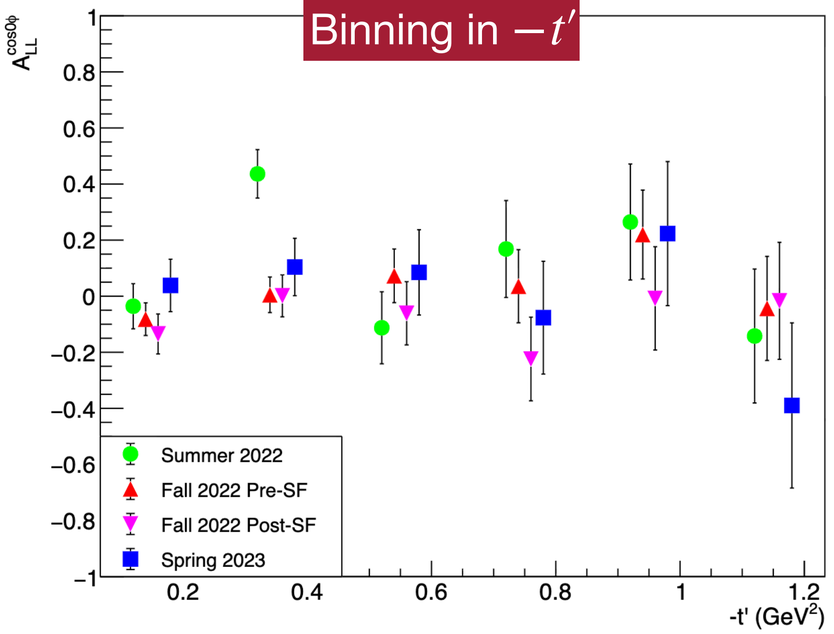

RG-C π^+ $F_{LL}^{\cos n\phi}/F_{UU}$, $0.1 \leq x_B < 0.25$

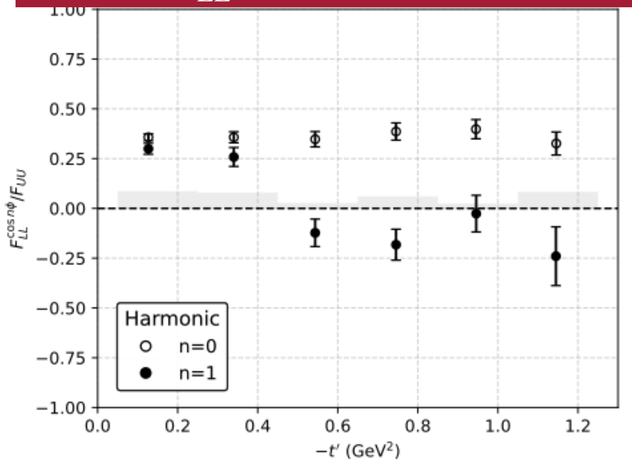

RG-C π^+ $F_{LL}^{\cos n\phi}/F_{UU}$, $0.45 \leq x_B < 0.6$

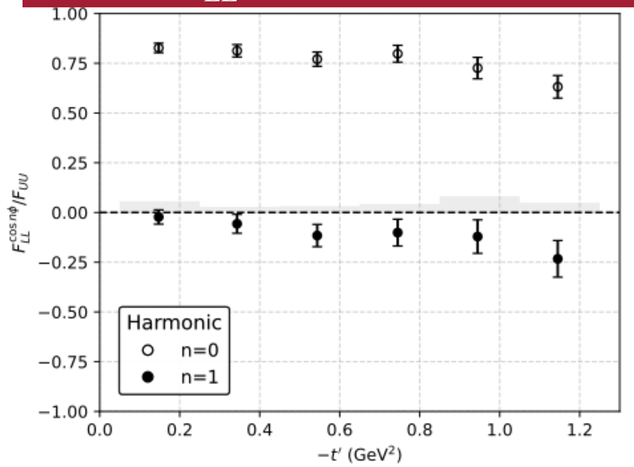

- Again, $A_{LL}^{\cos 0\phi}$ results are consistent between run periods and fairly stable as a function of x_B and $-t'$ (within very large uncertainty) → similar to π^+ $A_{LL}^{\cos 0\phi}$
- Possibly larger $A_{LL}^{\cos 0\phi}$ in smallest x_B bin, in which case π^- and π^+ $A_{LL}^{\cos 0\phi}$ would behave inversely as a function of x_B
- Results appear to be much smaller than π^+ $A_{LL}^{\cos 0\phi}$ in general

$A_{LL}^{\cos\phi}$ for 1D x_B and 1D $-t'$ Binning

Binning in x_B

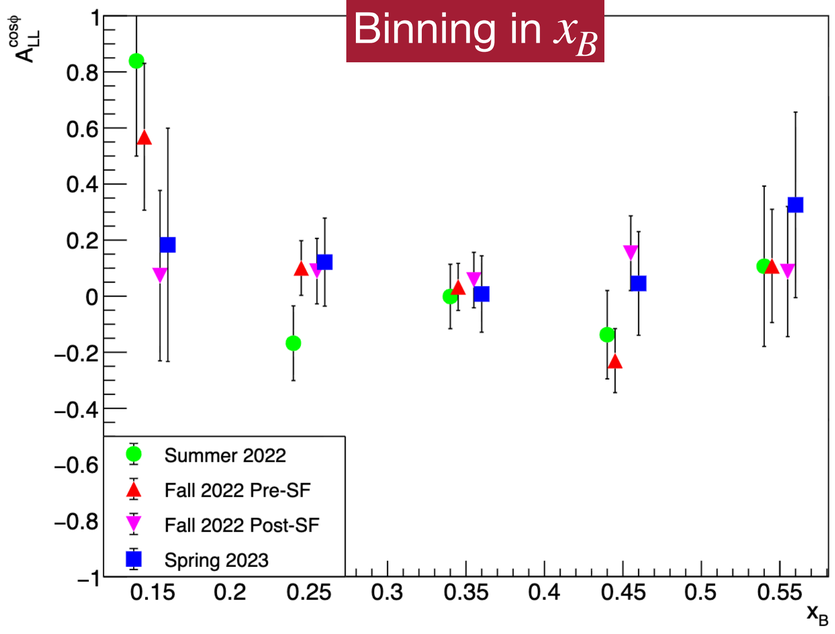

Binning in $-t'$

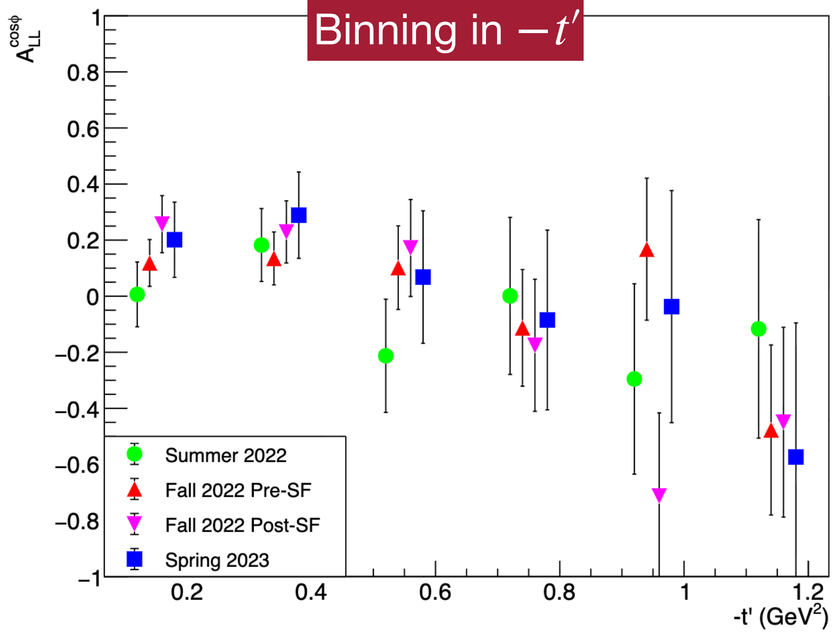

RG-C π^+ $F_{LL}^{\cos n\phi}/F_{UU}$, $0.1 \leq x_B < 0.25$

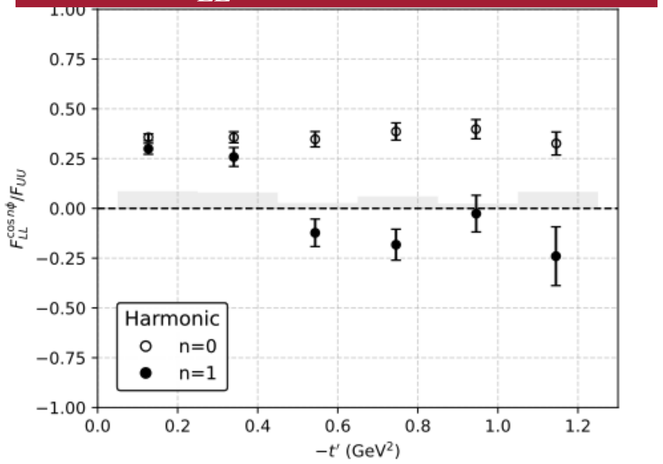

RG-C π^+ $F_{LL}^{\cos n\phi}/F_{UU}$, $0.45 \leq x_B < 0.6$

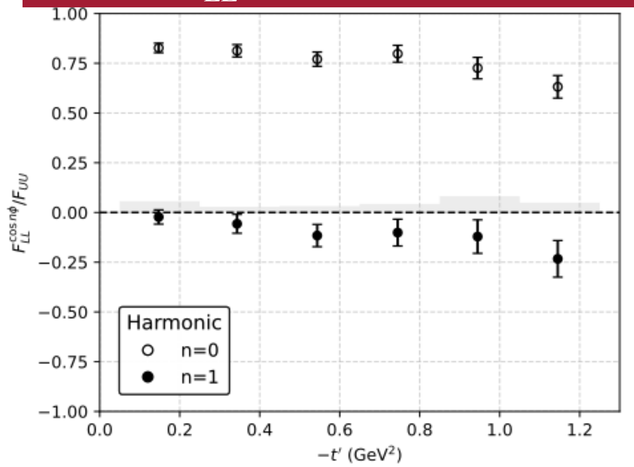

- Again, $A_{LL}^{\cos\phi}$ results are consistent between run periods within at times very large uncertainty
- As a function of x_B, $A_{LL}^{\cos\phi}$ appears to be mostly stable
- $A_{LL}^{\cos\phi}$ trends increasingly negative as a function of $-t' \rightarrow$ similar behaviour to π^+ $A_{LL}^{\cos\phi}$

Depolarization Factors

- From $A_{LU}^{\sin\phi}$, $A_{UL}^{\sin\phi}$, $A_{UL}^{\sin 2\phi}$, $A_{LL}^{\cos 0\phi}$, and $A_{LL}^{\cos\phi}$, extract structure function ratios using depolarization factors (typical for comparison with theory):

$$A_{LU}^{\sin\phi} = \left(\frac{W}{A}\right)\left(\frac{F_{LU}^{\sin\phi}}{F_{UU}}\right) \quad A_{UL}^{\sin\phi} = \left(\frac{V}{A}\right)\left(\frac{F_{UL}^{\sin\phi}}{F_{UU}}\right) \quad A_{UL}^{\sin 2\phi} = \left(\frac{B}{A}\right)\left(\frac{F_{UL}^{\sin 2\phi}}{F_{UU}}\right)$$

$$A_{LL}^{\cos 0\phi} = \left(\frac{C}{A}\right)\left(\frac{F_{LL}^{\cos 0\phi}}{F_{UU}}\right) \quad A_{LL}^{\cos\phi} = \left(\frac{W}{A}\right)\left(\frac{F_{LL}^{\cos\phi}}{F_{UU}}\right)$$

$$\epsilon = \frac{1 - y - \frac{1}{4}\gamma^2 y^2}{1 - y + \frac{1}{2}y^2 + \frac{1}{4}\gamma^2 y^2}$$

$$A(\epsilon, y) = \frac{y^2}{2(1-\epsilon)} \quad B(\epsilon, y) = \frac{y^2\epsilon}{2(1-\epsilon)} \quad C(\epsilon, y) = \frac{y^2\sqrt{1-\epsilon^2}}{2(1-\epsilon)}$$

$$V(\epsilon, y) = \frac{y^2\sqrt{2\epsilon(1+\epsilon)}}{2(1-\epsilon)} \quad W(\epsilon, y) = \frac{y^2\sqrt{2\epsilon(1-\epsilon)}}{2(1-\epsilon)}$$

Binning in x_B

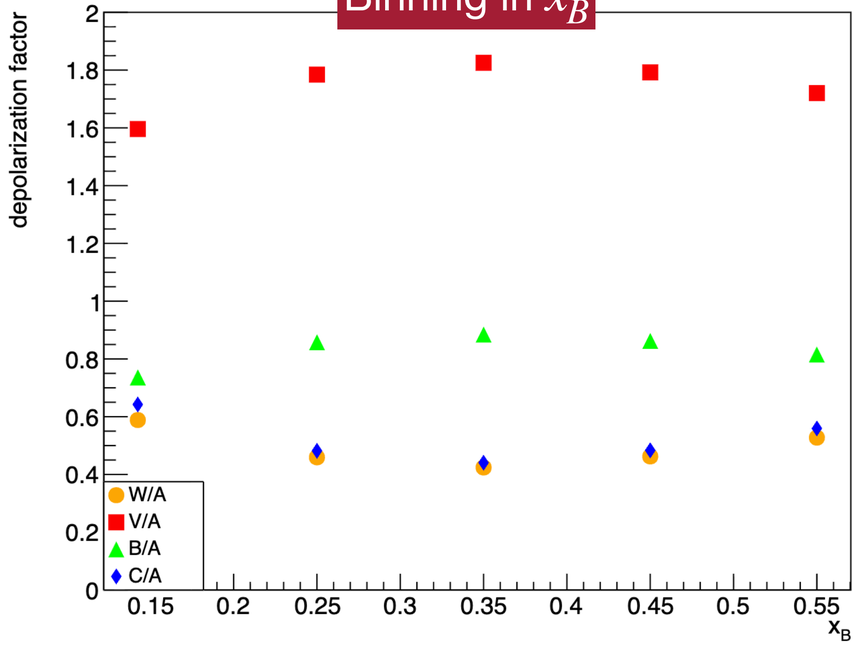

Binning in $-t'$

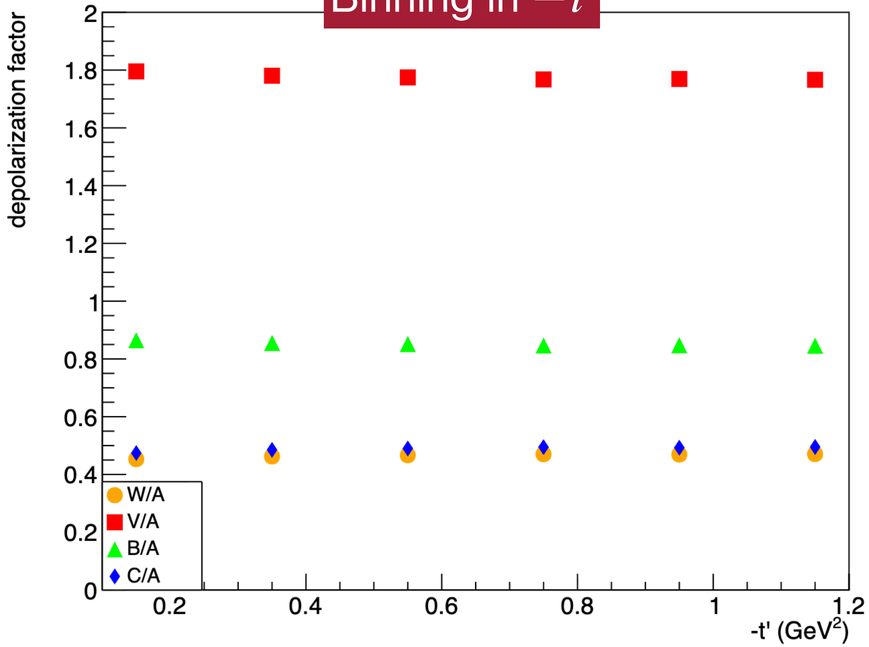

Depolarization factors' dependence on x_B and $-t'$ using Fa22 Pre-SF data

Conclusions and Next Steps

- ✓ Studying exclusive π^- data from RG-B and RG-C → beam spin asymmetry results from RG-B are interesting as both and independent measurement and as a cross check to RG-C results
- ✓ Refined cuts to better select exclusive π^- events interacting with neutrons bound in deuterons for ND_3 (LD_2) target
- ✓ Beam spin asymmetries extracted binned up to 2D in $\left(x_B, -t'\right)$, with overall good agreement in kinematic bins between RG-C run periods and RG-B
- ✓ Extraction of target spin asymmetry and double spin asymmetry for RG-C run periods in 1D for x_B and $-t'$ → great agreement between run periods with large uncertainty bars
- Given good agreement between RG-C run periods, interested to see improvements on statistical uncertainty after combining run periods, hopefully more interpretable results
- Systematic studies similar to those performed on RG-C DVπ^+P analysis needed (currently quality, PID cuts, etc. are quite minimal)

Thank you, questions?

Backup Slides

Full Kinematic Definition of $-t'$

$$t' = t - t_{min}$$

$$t_{min} = \frac{Q^2(2(1-x_B)(1-\sqrt{1+\epsilon^2})+\epsilon^2}{4x_B(1-x_B)+\epsilon^2} 4M^2x_B^2/Q^2$$

$$\epsilon^2 = 4M^2x_B^2/Q^2$$

Summer 2022 Yields

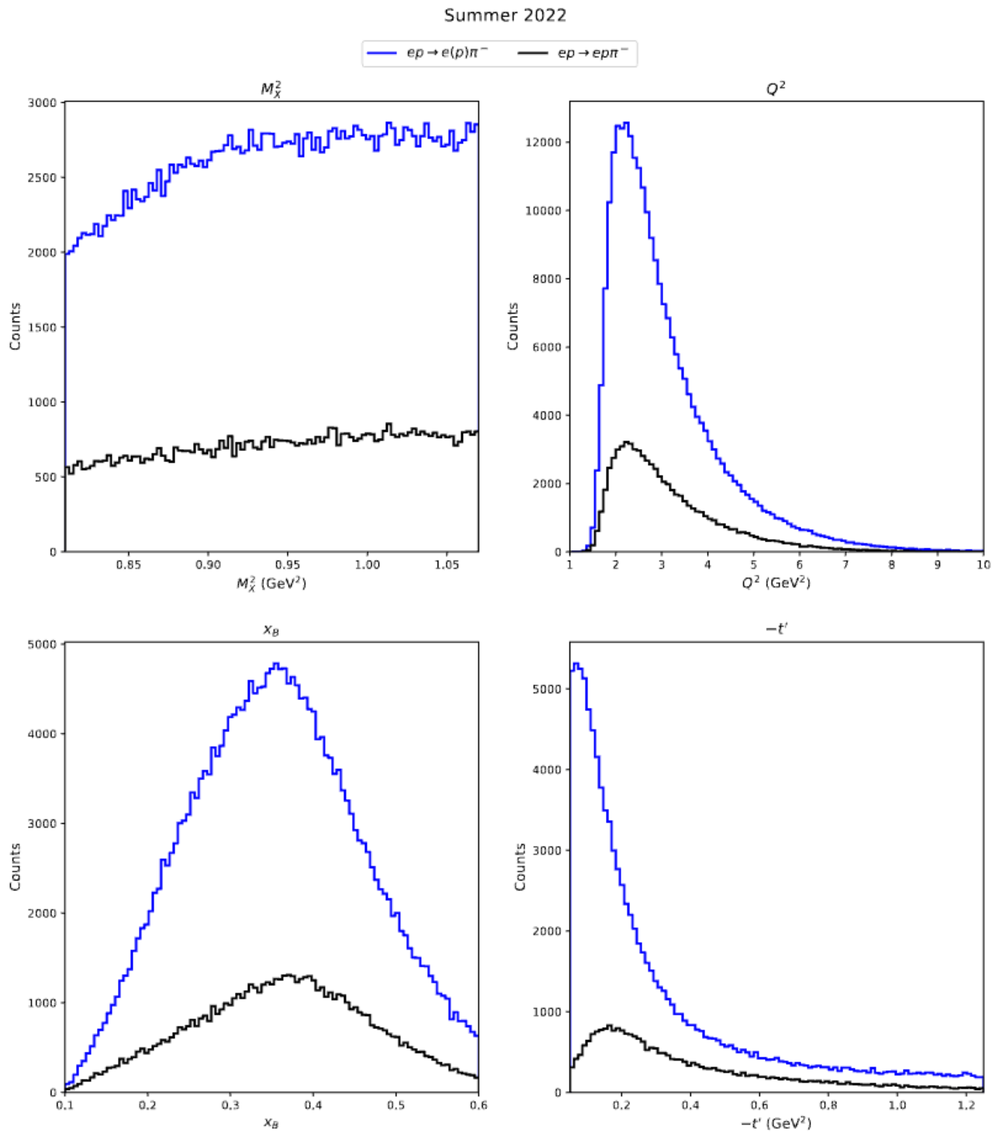

Fall 2022 Yields

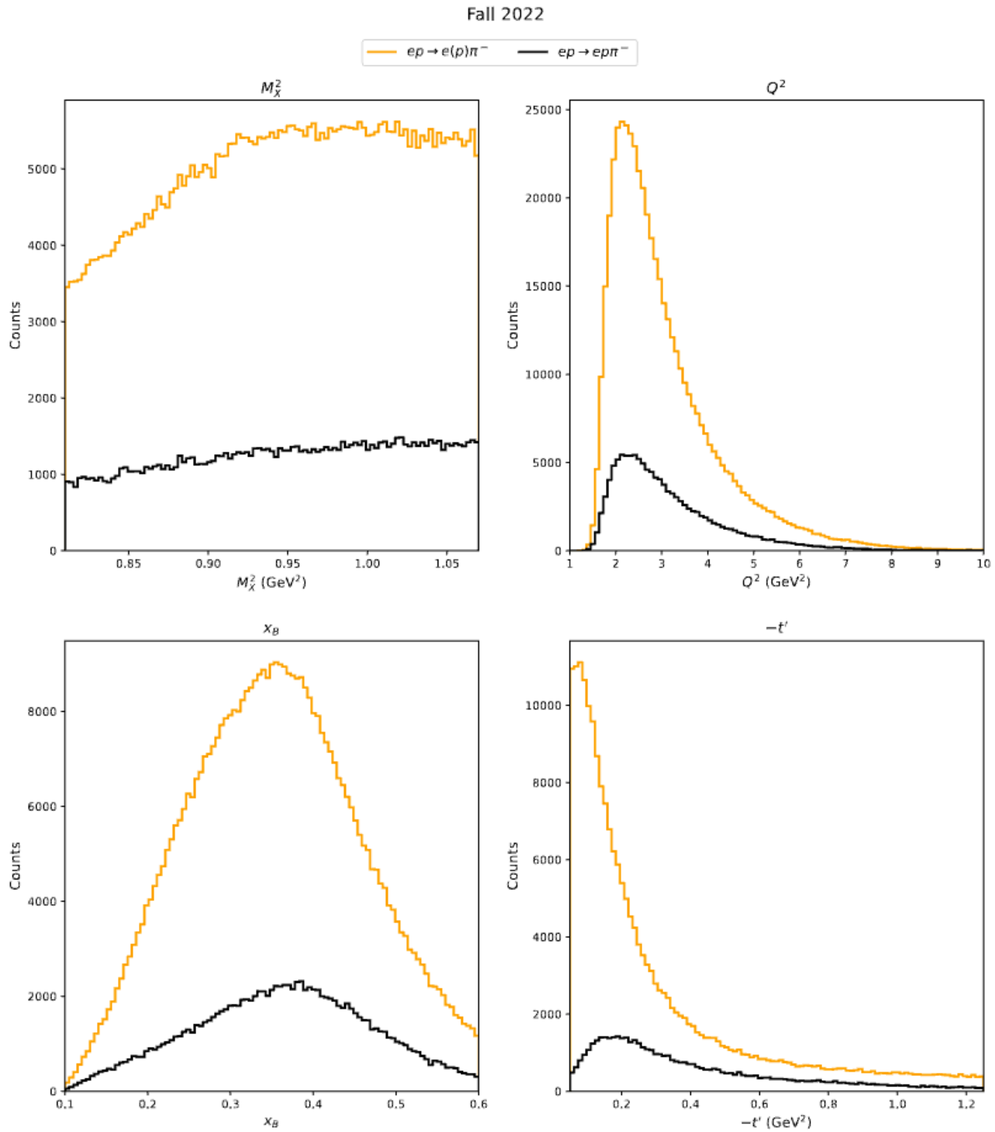

Spring 2023 Yields

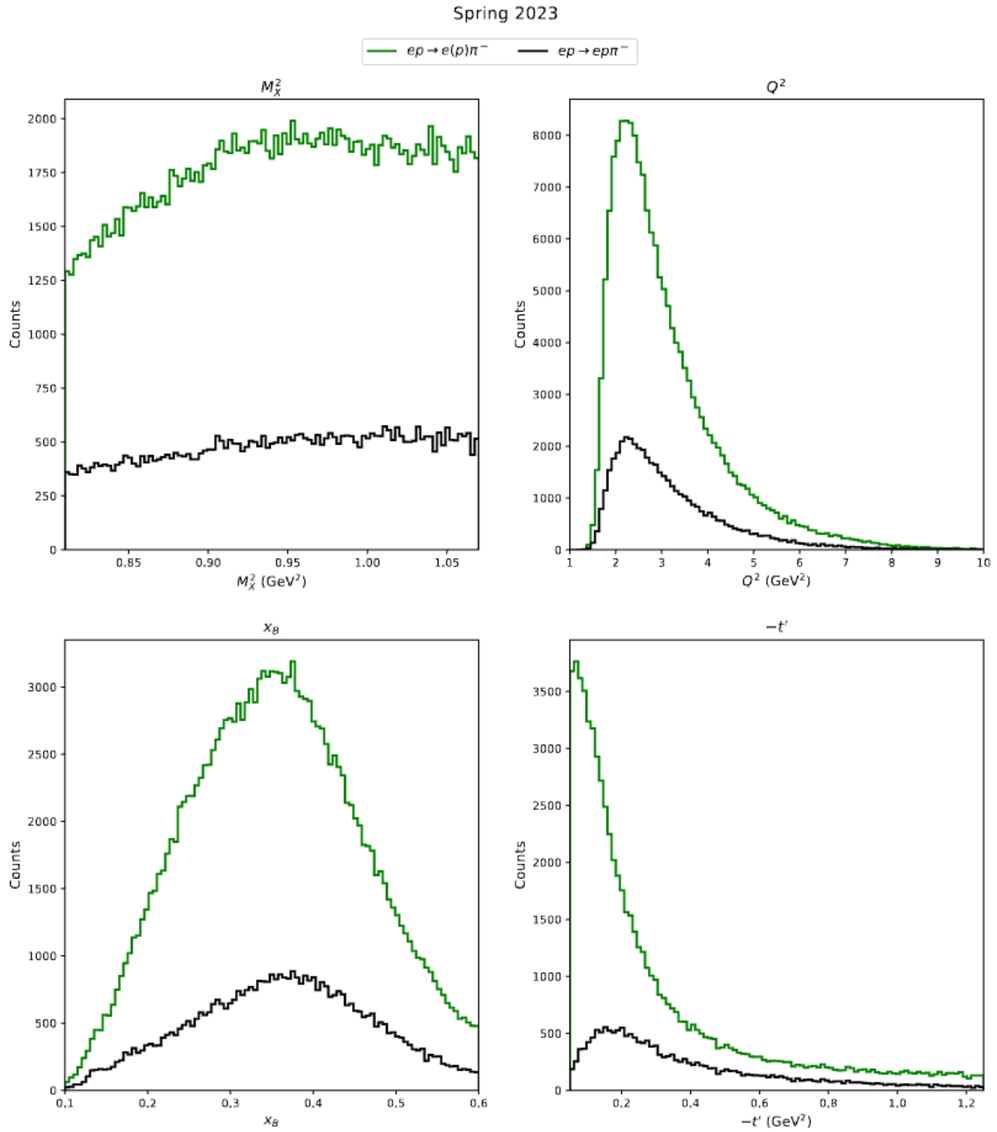

Alternate calculations for $-t \rightarrow -t'$

$\Delta t = \left(p - p'\right)^2 - \left(q - p_\pi\right)^2$ distributions for RG-C Fa22, on ND_3 (nuclear target with heightened Fermi motion)

$t' = t - t_{min}$

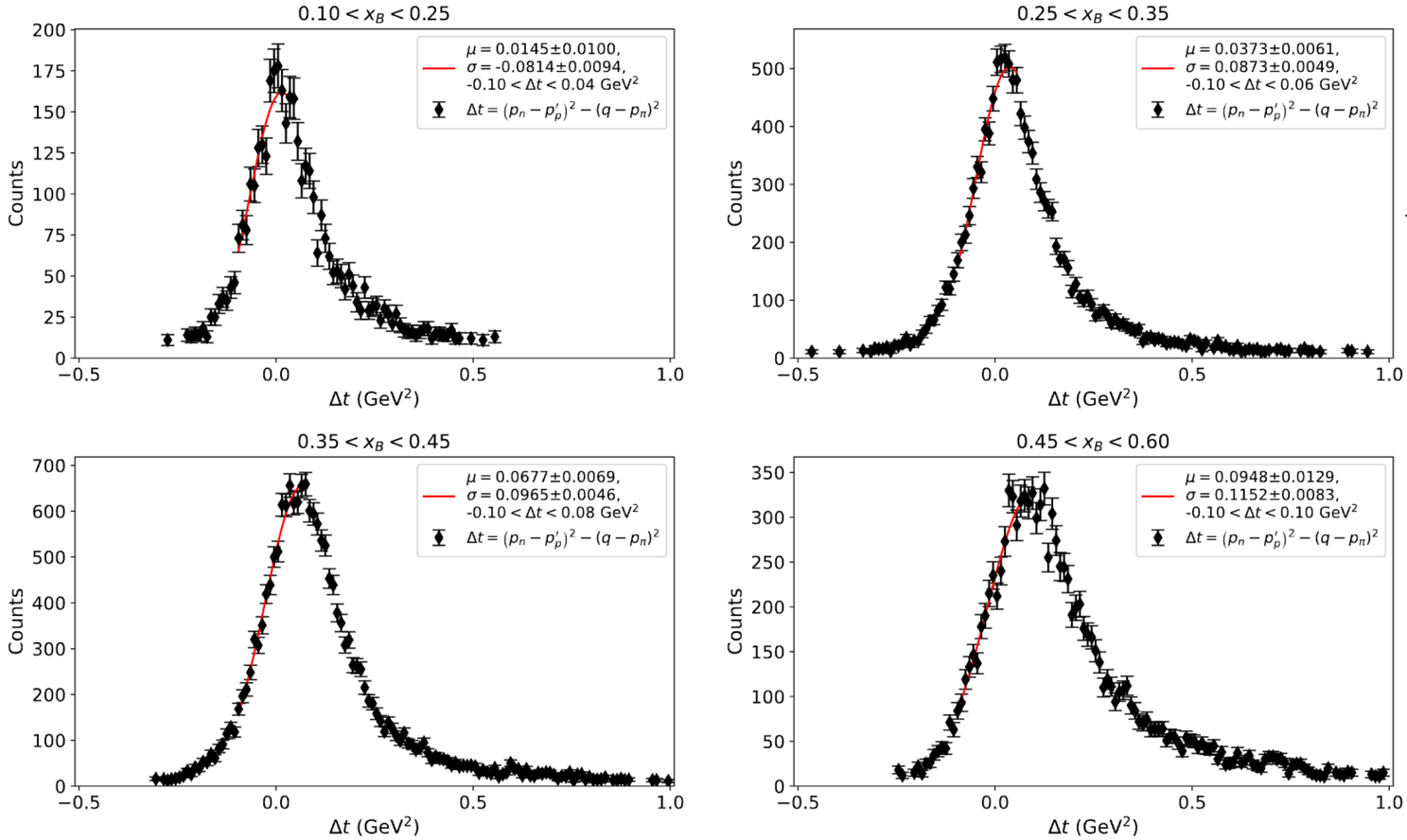

← width of distributions enhanced by Fermi motion, these are likely events occurring off nitrogen

→ How we use kinematics accessible with three particle final state to constrain Fermi motion?

Cone angle cut

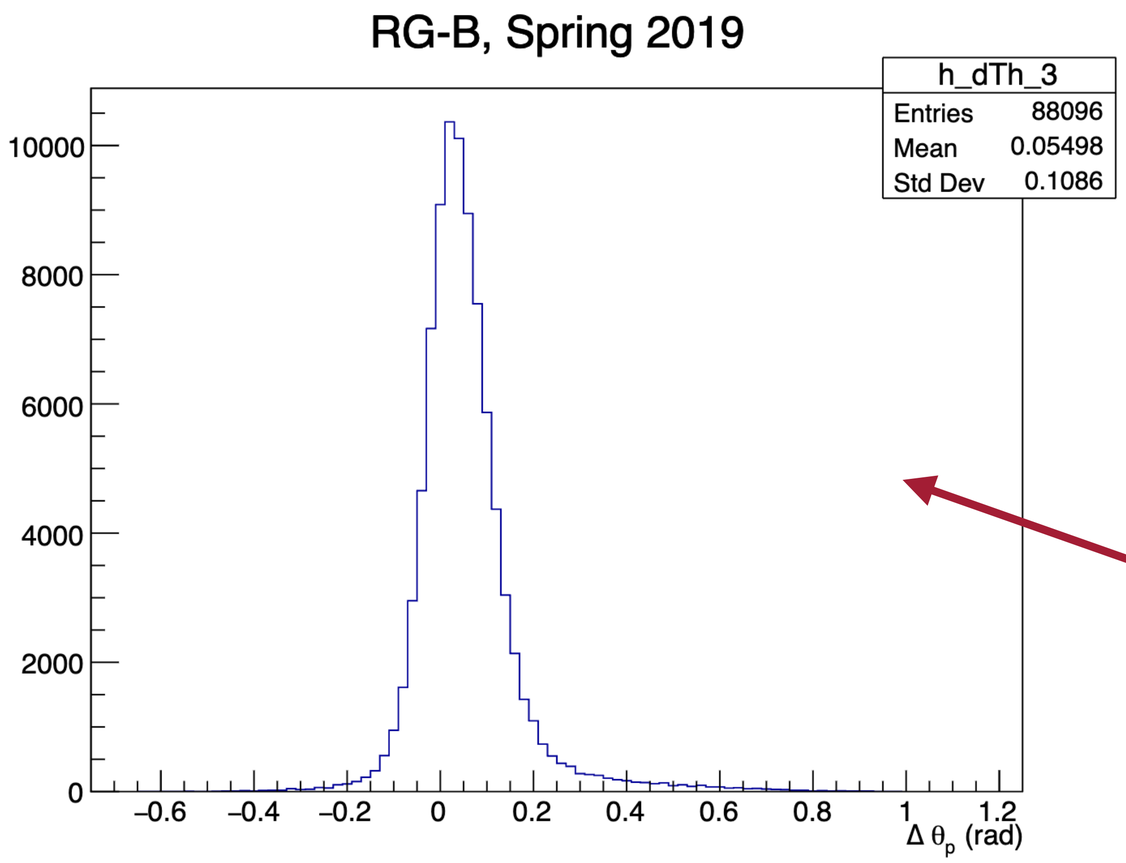

- Measuring difference between detected and reconstructed (using π^- and e^-) proton θ
- When calculating proton 4-vector, we assume no Fermi motion
- Discrepancy provides insight on Fermi motion contributions
- Can use RG-B as baseline for expected distribution from deuterons (unpolarized LD_2 target)

RG-B Sp19
$\mu = 0.05496$
$\sigma = 0.1086$

vs.

RG-C
$\mu \sim 0.24$
$\sigma \sim 0.27$

→ RG-B data helps us define a cone angle cut to select events off of deuterons for RG-C (RG-B $\mu \pm \sigma$)

Alternate calculations for $-t \rightarrow -t'$

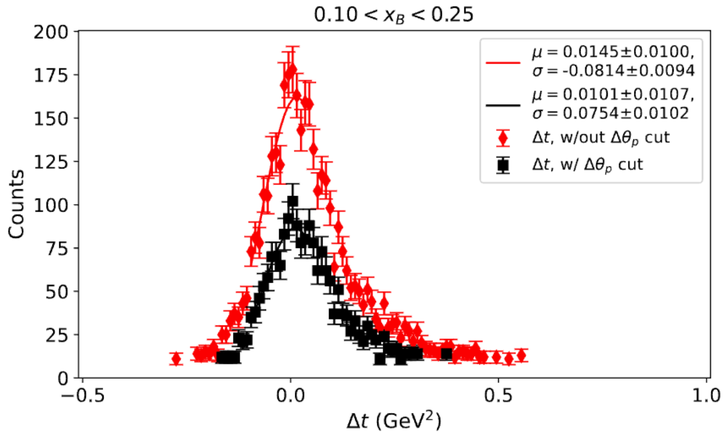

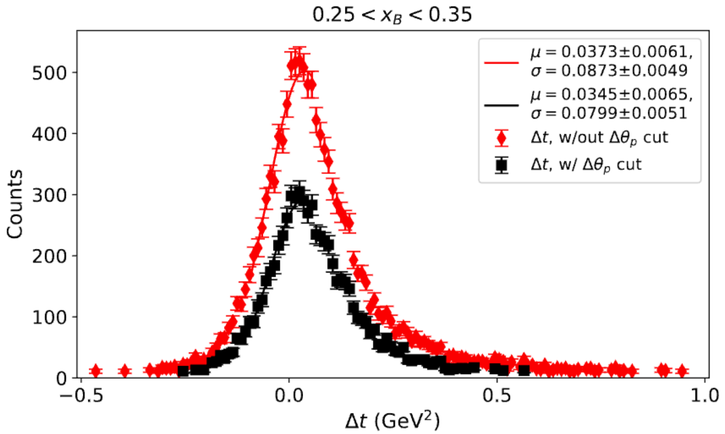

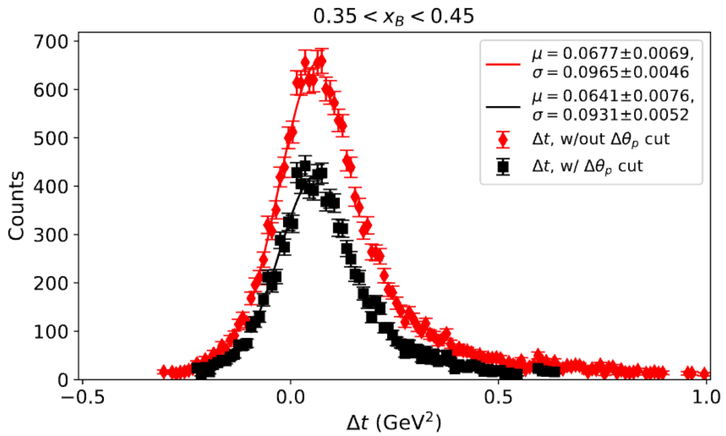

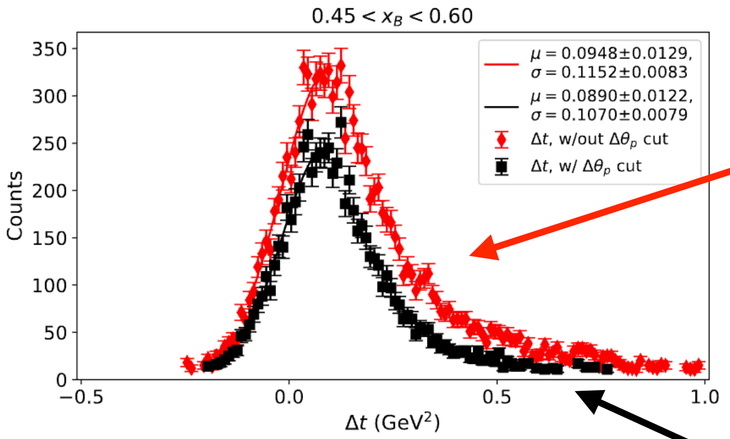

Constraining $\Delta\theta_p$ narrows Δt distribution, removing events identified as being nuclear in origin due to high Fermi motion

without $\Delta\theta_p$ cut

with $\Delta\theta_p$ cut

Alternate calculations for $-t \rightarrow -t'$

Still not as narrow as RG-B Δt distributions!

RG-C Fa22, on ND_3

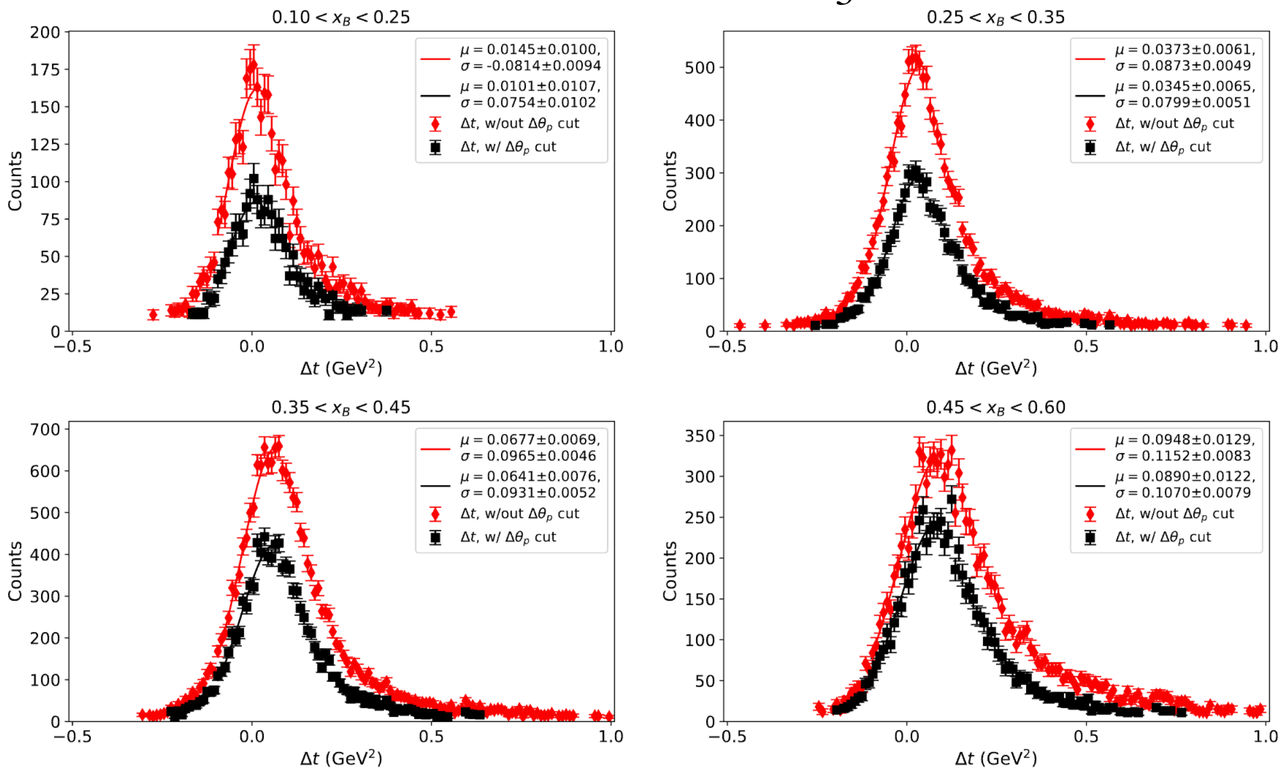

RG-B Sp19, on LD_2

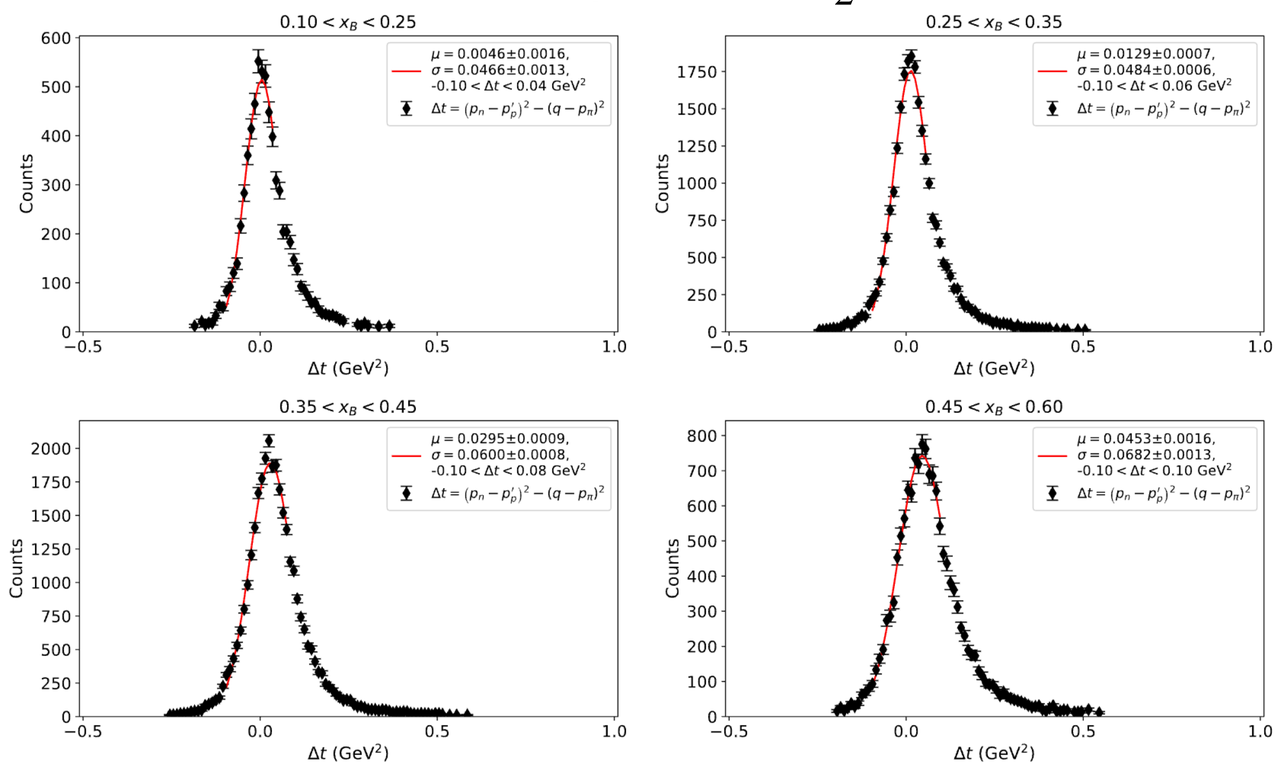

$\rightarrow \Delta\theta_p$ cuts removes some Fermi motion effects, but not all (other effects as well)

Summer 2022 Δt

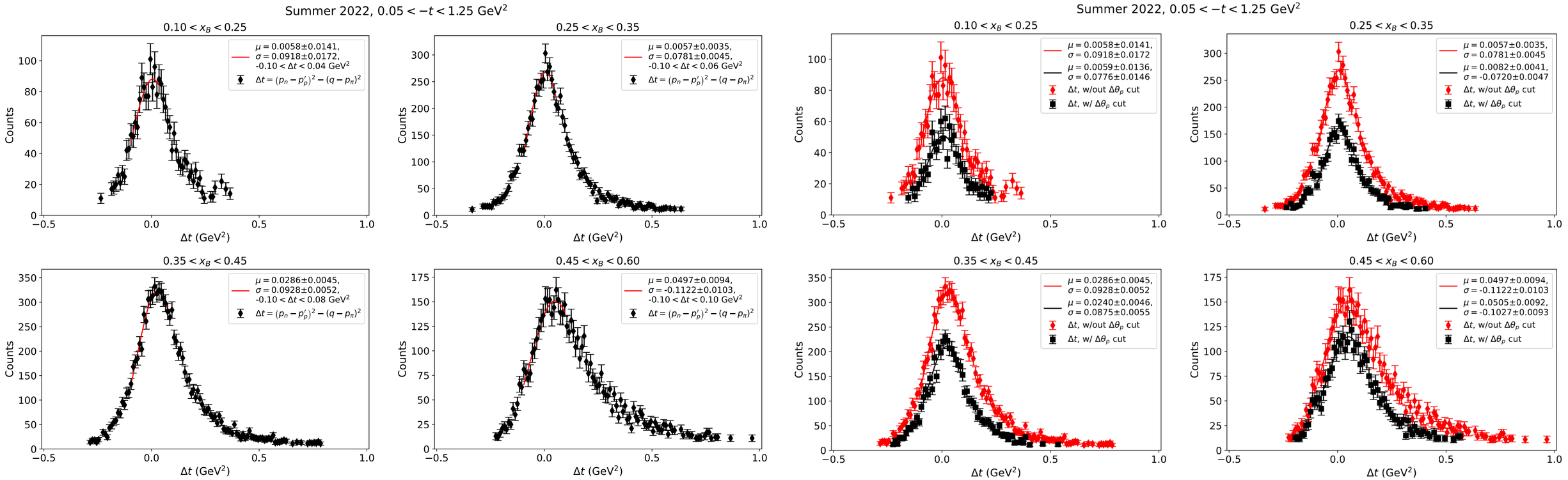

Fall 2022 Δt

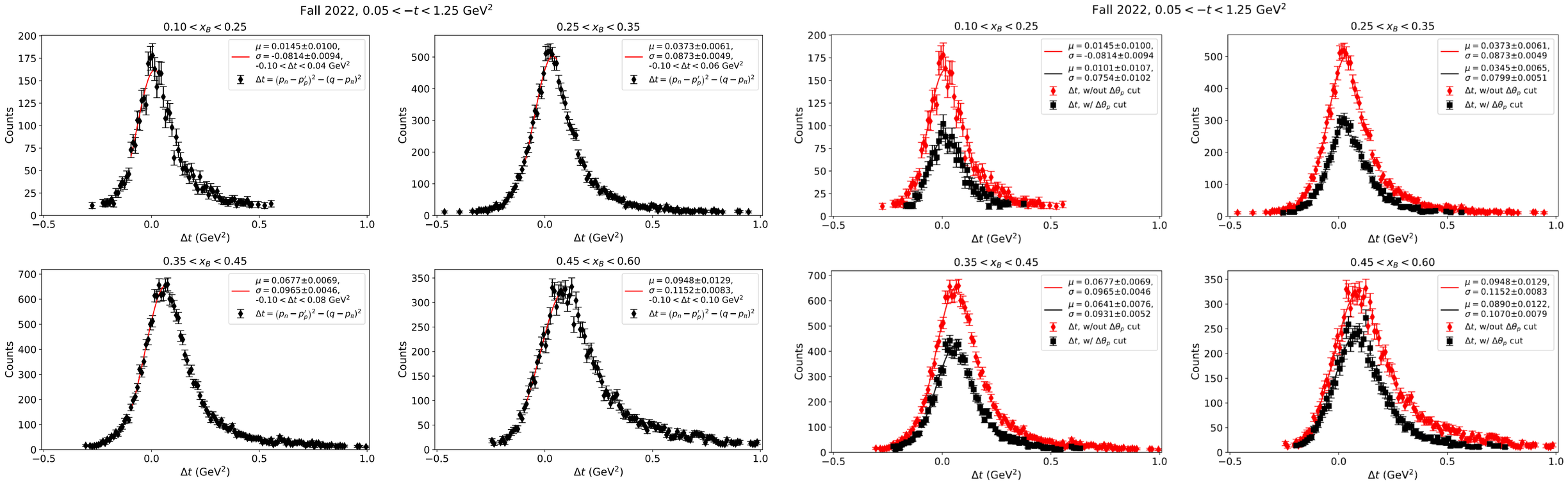

Spring 2023 Δt

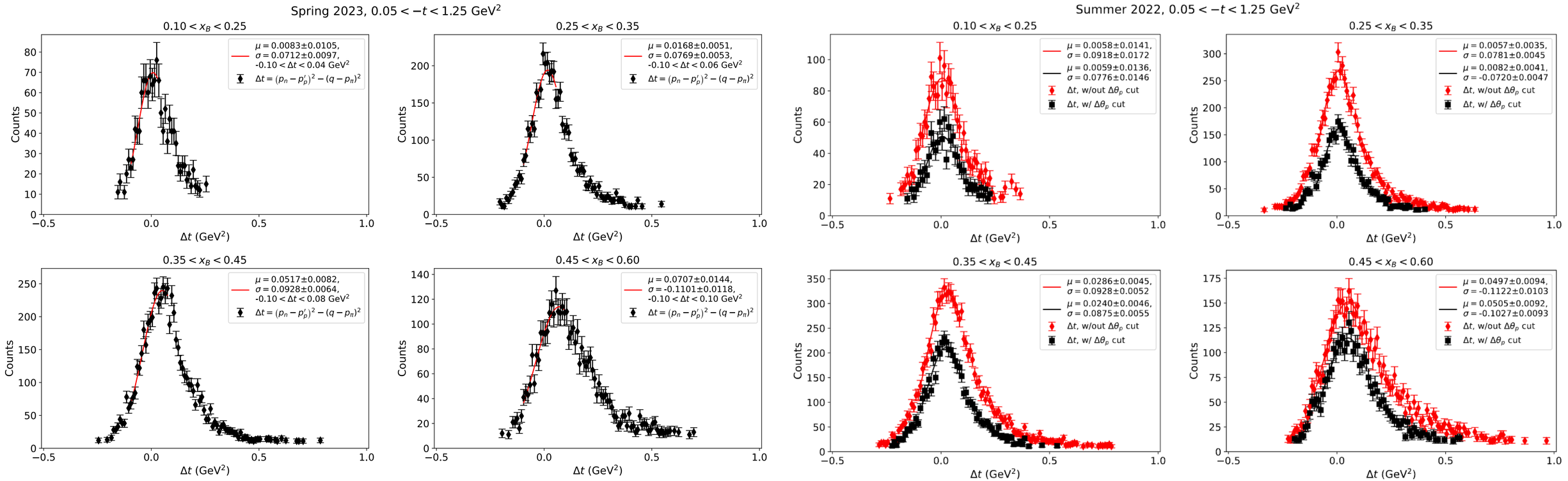

Alternate calculations for $-t \rightarrow -t'$

Direct comparison using fits to Gaussian:

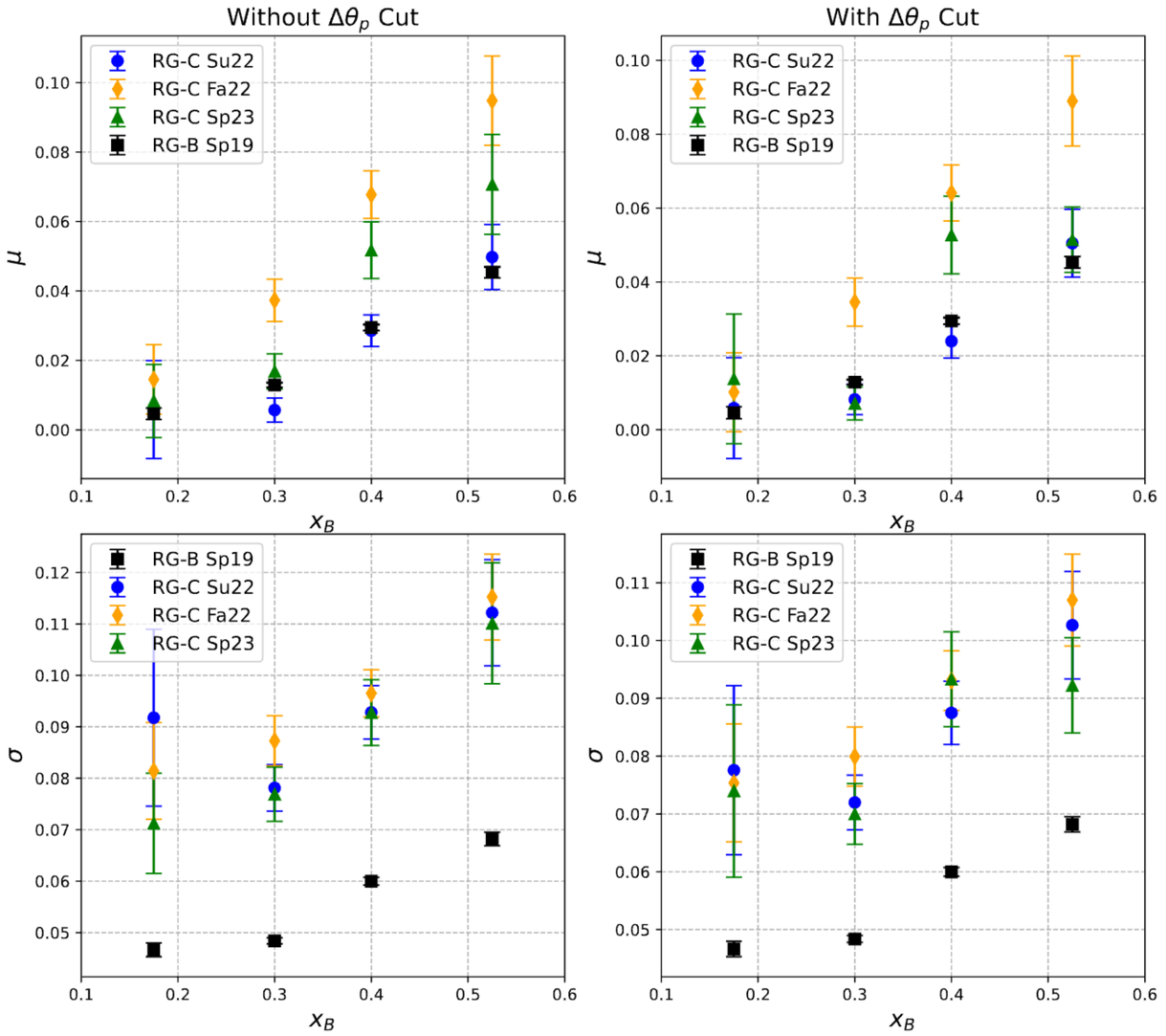

→ μ: resolution of "reconstructed" t; relatively consistent (using same CLAS12 detectors)

→ σ: Fermi motion; clear differences between RG-B and RG-C, even with $\Delta\theta_p$ cut

Alternate dilution factor calculation techniques

$$DF = \frac{(n_A - n_{MT})\,(n_{CD} - 0.757666 n_C - 0.005200 n_{MT} - 0.237132 n_F)}{n_A\,(n_{CD} - 0.168370 n_C - 0.865973 n_{MT} + 0.03434 n_F)}$$

vs.

$$DF = 2.260129 \frac{PF}{n_A}\,(n_{CD} - 0.757666 n_C - 0.005200 n_{MT} - 0.237132 n_F)$$

shown for $en \rightarrow e(p)\pi^-$

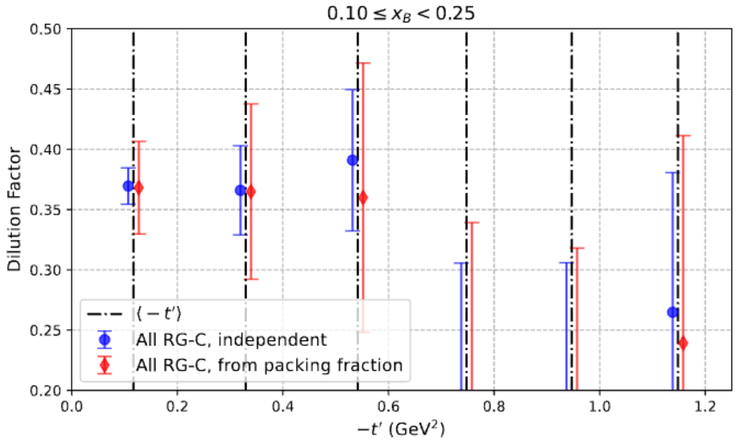

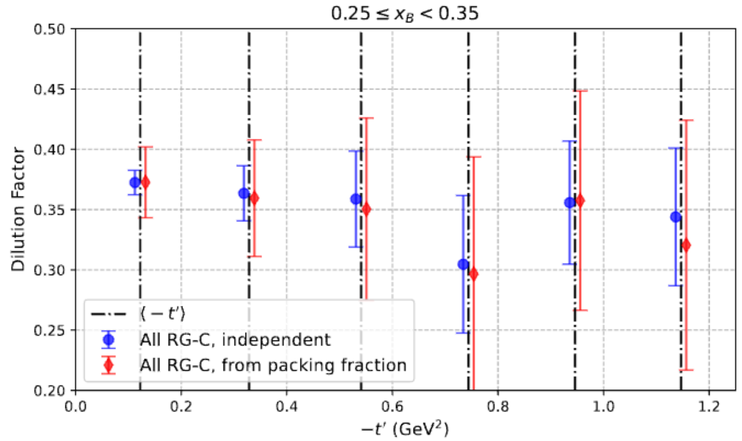

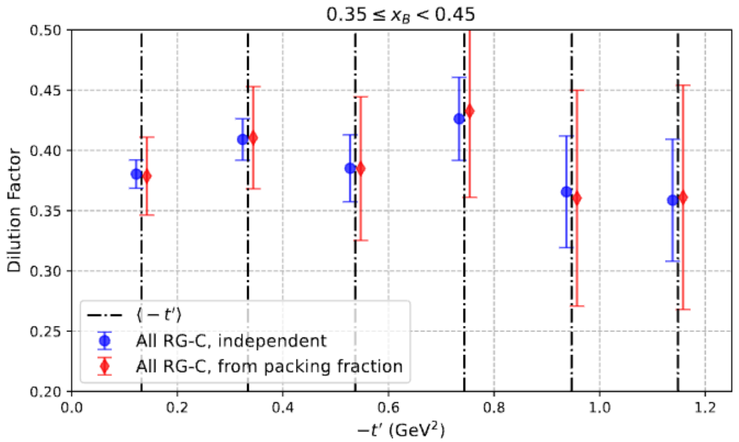

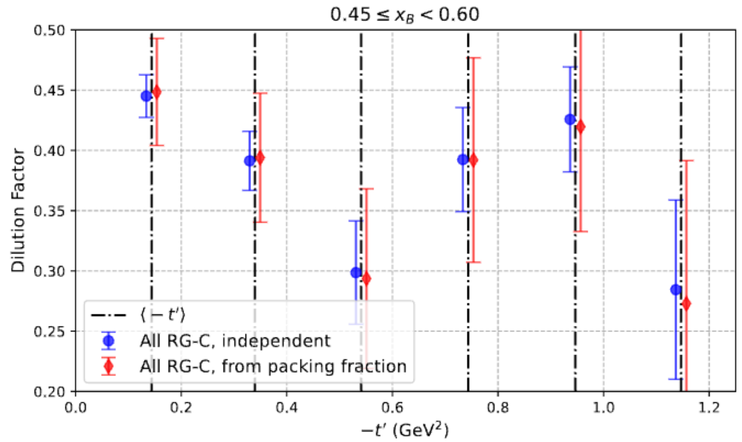

Packing fraction studies

Also useful to extract packing fraction of each run period epoch to measure consistency, shown here without M_X^2 cuts for larger sample size

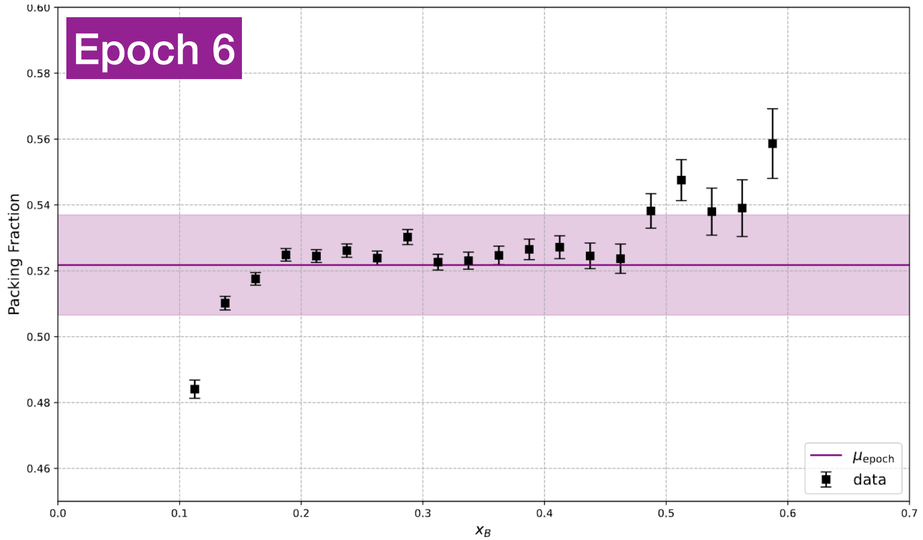

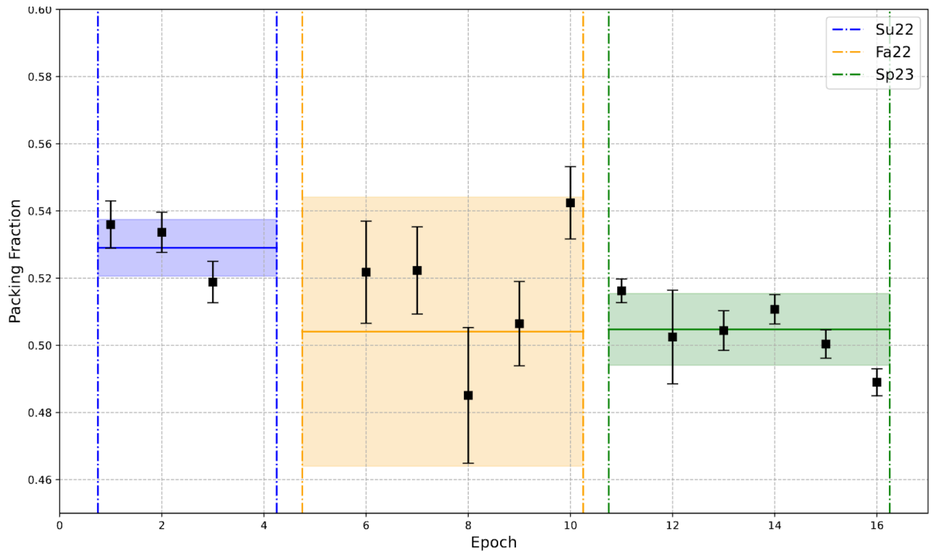

Individual epoch, $Pf(x_B)$

Averages across all epochs in run-period

→ Still a work in progress to get perfect agreement in epoch packing fraction results across run group, but in general consistent to order of ~5%

Comparing exclusive π^+ BSAs from RG-A and RG-C

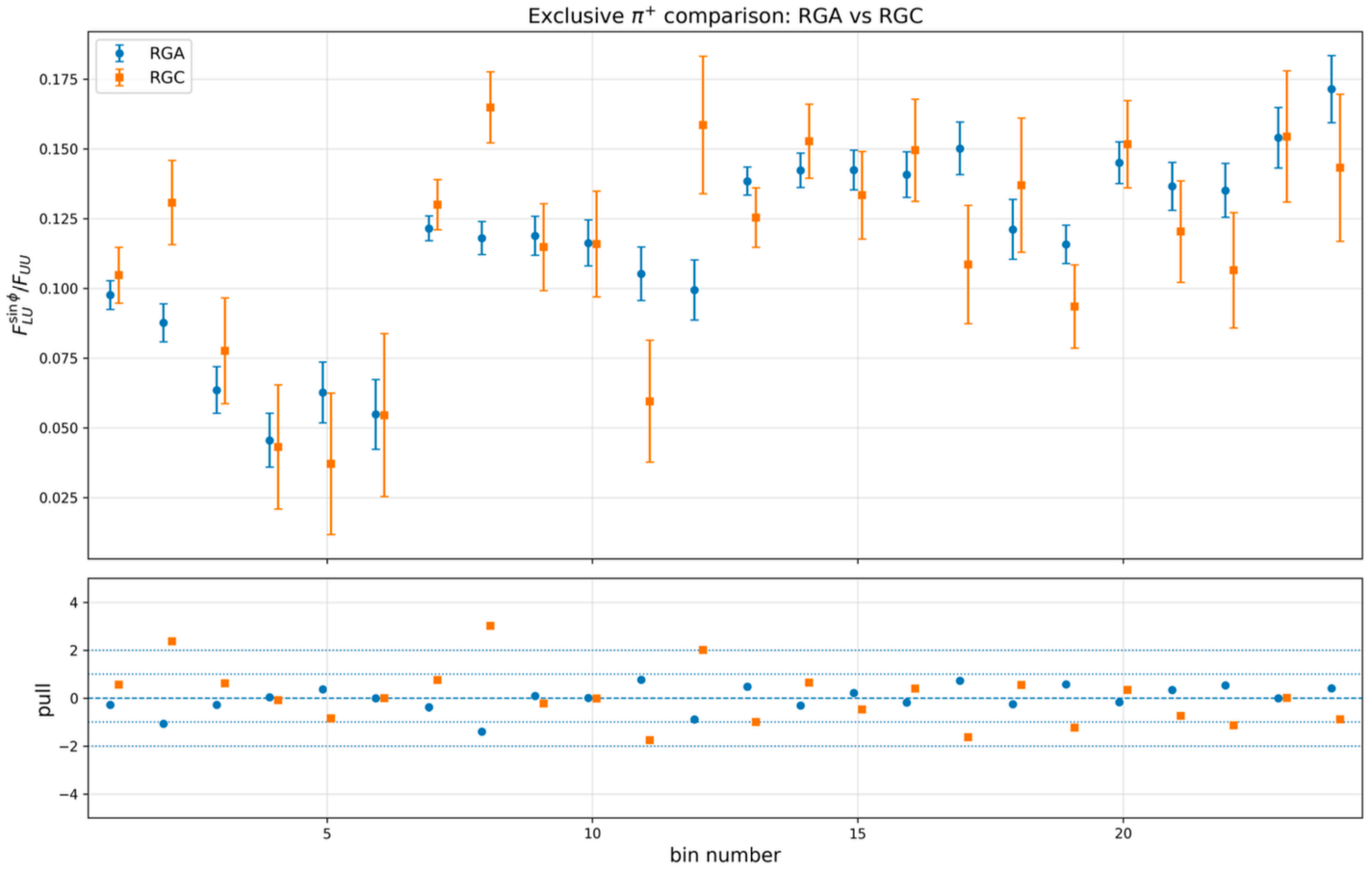

Figure 70: Comparison of the $F_{LU}^{\sin\phi}/F_{UU}$ structure function ratio for measurements off the liquid hydrogen target in RGA and the solid ammonia target in RGC for all 24 kinematic bins measured in this analysis. The mean residual of the RGC result with respect to RGA is -0.001 and the mean absolute value of the pulls are 1.074.

HERMES Comparison

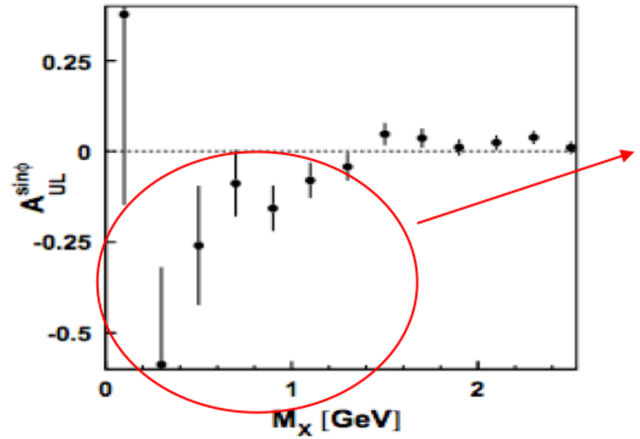

- The low statistics measurement from HERMES shows a large negative asymmetry in the exclusive region.
- CLAS(12) BSA measurements had shown positive asymmetry.
- Traditionally BSA ~ TSA.

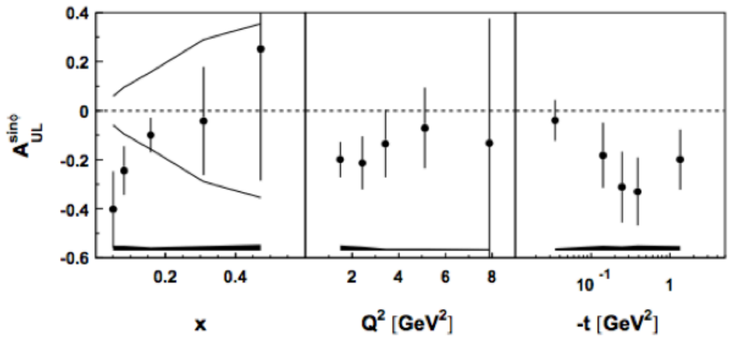

Phys.Lett.B 535 (2002) 85-92 [hep-ex/0112022]

- Similarly, measurements for exclusive π^+ and π^- were shown to have the same sign.

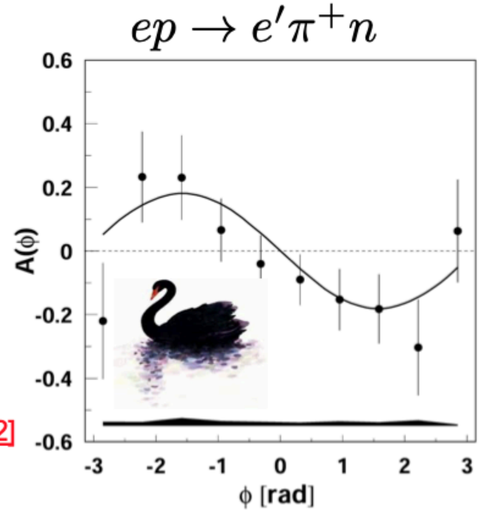

Phys.Lett.B 562 (2003) 182-192 [hep-ex/0212039]

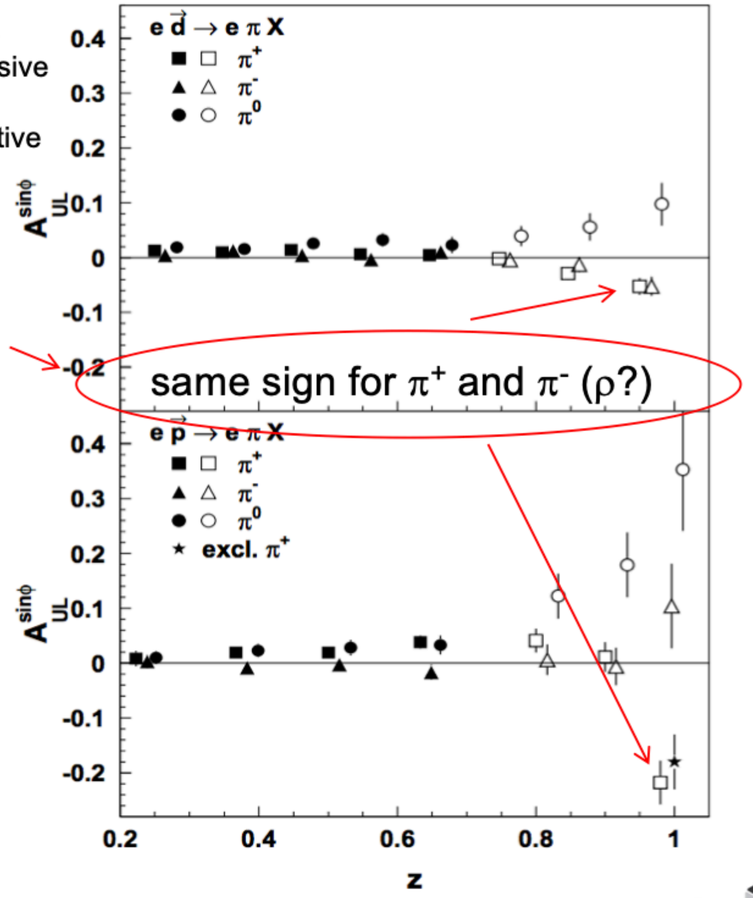

Slide from T. Hayward, https://indico.jlab.org/event/990/contributions/17920/attachments/13540/21860/Hayward_exclusive_meson_RGC.pdf

π^- Structure Function Predictions from Peter Kroll